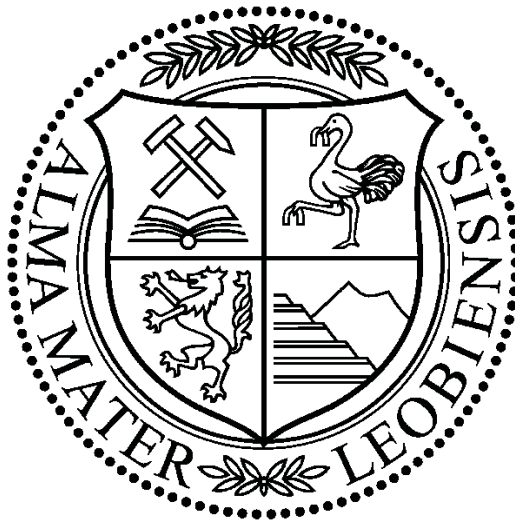


Master Thesis

DESIGN OF A NEW PUMP JACK FOR CONTINUOUS SUCKER ROD PUMPING SYSTEMS



Written by:

Maher HADJ AHMED HILALI
1435533

Advisors:

Fazeli Tehrani, Fatemeh, Dipl.-Ing.
Hofstätter, Herbert, Univ.-Prof. Dipl.-Ing. Dr.mont.

Leoben, 04/06/2018

EIDESSTATTLICHE ERKLÄRUNG

Ich erkläre an Eides statt, dass ich die vorliegende Masterarbeit selbständig und ohne fremde Hilfe verfasst, andere als die angegebenen Quellen und Hilfsmittel nicht benutzt und die den benutzten Quellen wörtlich und inhaltlich entnommenen Stellen als solche erkenntlich gemacht habe.

AFFIDAVIT

I hereby declare that the content of this work is my own composition and has not been submitted previously for any higher degree. All extracts have been distinguished using quoted references and all information sources have been acknowledged.

Acknowledgement

First, I would like to express my sincere gratitude to Professor Herbert Hofstätter for offering me the opportunity to work on this interesting topic and for his continuous support and valuable recommendations during the course of this project.

I would also like to express my thankfulness to my thesis advisor Mrs. Fatemeh Fazeli for always having the door open whenever I ran into a trouble spot or had a question about my research or writing. She consistently steered me in the right direction whenever she thought I needed it.

Finally, I must express my very profound gratitude to my parents, my family members and to my beloved friends for providing me with unfailing support and continuous encouragement throughout my years of study and through the process of researching and writing this thesis. This accomplishment would not have been possible without them. Thank you.

Kurzfassung

Das Verwenden von Tiefpumpen/Pferdekopfpumpen ist die am weitesten verbreitetste künstliche Fördermethode für Erdöl- und Erdgasbohrungen. Eine der Komponenten an der Oberfläche dieser Baueinheit ist der Pferdekopf, welcher verwendet wird um die Pendelbewegung auf die Kolbenstange und das Pumpengestänge zu übertragen. Jedoch wird die traditionelle Trägereinheit einem Überdrehmoment und einer strukturellen Belastung unterworfen, was sich drastisch schädigend auswirken kann. Desweiteren stellen konventionelle Pferdeköpfe in Bezug auf Energieverbrauch, großer Standfläche, Hublänge und Geschwindigkeitskontrolle eine große Herausforderung dar. Folglich können hydraulische Pump-Einheiten als Alternative zu traditionellen Pferdeköpfen betrachtet werden, da diese den Förderbetrieb verbessern sowie Energieanforderungen und HSE-Bedenken reduzieren können.

In dieser Arbeit werden zunächst unterschiedliche Fördereinheiten untersucht und in weiterer Folge analysiert. Angeregt von diesen Technologien wurde eine weitere „energiesparende“ hydraulische Einheit mithilfe von MatLab/Simulink entworfen. Verschiedene von einander unabhängige Einheiten wurden entworfen, um die Leistung zu optimieren und den Energieverbrauch zu reduzieren. Die Einheit wurde danach simuliert um sowohl eine Seilzugstange als auch ein konventionelles Pumpengestänge zu aktivieren. Deren Leistung wurde im Anschluss mit einem äquivalenten Szenarium, das einen konventionellen Pferdekopf beinhaltet, verglichen.

Die Ergebnisse zeigen, dass die entworfene Einheit eine genauere Steuerung des Förderkreislaufes hinsichtlich der Fördergeschwindigkeit und der Hublänge zulässt. Der Energieverbrauch der Einheit führt, trotz der höheren Förderaktivität bzw. Pumpentätigkeit und der größeren Produktivität, ebenfalls, verglichen mit konventionellen Tiefpumpen/Pferdekopfpumpen, die den gleichen Bohrlochbedingungen ausgesetzt sind, zu deutlich besseren Ergebnissen.

Schlagwörter: Hübe pro minute ; drahtseil ; Energy verbrauch ; Grundfläche ; Hublänge ;Hydraulik pumpenaggregat ; Gestängepumpe ; Pumpe Heber

Abstract

Sucker rod pumping is the most widely used artificial lift method in oil and gas wells. The surface component of this unit is the pump jack, which is designated to impart the reciprocating motion onto the polished rod and rod string. However, traditional beam unit is subjected to over torque and structural loading which can be drastically damaging. Moreover, conventional pump jacks pose many challenges in terms of energy consumption, large footprint, stroke length and speed control. Hence, considering hydraulic pumping units as an alternative to traditional Pump jacks can improve the production operations and reduce energy requirements and HSE concerns.

In this thesis, different hydraulic pumping units are initially studied and analyzed. Inspired by these technologies, a hydraulic unit is designed and simulated using Simulink/Matlab software with the aim of saving input energy. Various components were independently designed to optimize the performance and reduce the energy consumption. The unit was then simulated to activate a wire rope string as well as a conventional sucker rod string and their performance were compared with equivalent scenarios using a conventional Pump jack. The results show that the unit allows for more precise control of the pumping cycle in terms of pumping speed and stroke length. The energy consumption of the unit is also compared to conventional sucker rod pumping units operating at the same wellbore conditions, leading to significantly better results despite the greater pumping activity and higher productivity.

Keywords: sucker rod pumping; pump jack ; hydraulic pumping unit ; stroke length ; wire rope; SPM ; energy consumption ; footprint

Table of Content

| | Page |
|--|-----------|
| 1 INTRODUCTION..... | 1 |
| 2 FUNDAMENTALS | 2 |
| 2.1 Artificial Lift Principles | 2 |
| 2.2 Sucker Rod Pumps | 3 |
| 2.2.1 Surface Equipment: | 4 |
| 2.2.2 Sucker Rod String | 5 |
| 2.2.3 Downhole Pump | 6 |
| 3 CONVENTIONAL SURFACE PUMPING UNITS | 9 |
| 3.1 Components of a Pumping Unit | 9 |
| 3.2 Pumping unit's designation | 9 |
| 3.3 Beam Pumping Units geometries..... | 10 |
| 3.3.1 Crank Balanced Pumping Units | 10 |
| 3.3.2 Beam-Balanced Pumping Units | 10 |
| 3.3.3 Air-Balanced Pumping Units | 11 |
| 3.3.4 Mark II Pumping Units..... | 12 |
| 3.3.5 Reverse Mark (RM) Pumping Unit | 12 |
| 3.4 Problems with Beam Pumping Units..... | 12 |
| 4 HYDRAULIC SURFACE PUMPING UNITS | 14 |
| 4.1 Hydraulic Pumping Unit using Gas Cylinder as Counterbalance (DynaPump)..... | 14 |
| 4.1.1 Operating Mechanism..... | 14 |
| 4.1.2 Power Unit..... | 16 |
| 4.1.3 Technical Description of the Unit..... | 16 |
| 4.1.4 Unit Kinematics..... | 17 |
| 4.2 Hydraulic Pumping Unit based on Electro-Hydraulic Proportional Control Technology | 18 |
| 4.2.1 Hydraulic System Design | 18 |
| 4.2.2 Speed Curve Design..... | 19 |
| 4.3 Energy-Saving Hydraulic Pumping Unit (HPU) | 20 |
| 4.3.1 Energy-Saving HPU Working Principle | 21 |
| 4.3.2 Speed Curve Design..... | 22 |
| 4.3.3 Parameter Analysis and Calculations of the Hydraulic Unit | 23 |

| | | |
|----------|---|-----------|
| 4.3.4 | Power Consumption under single Well Operation Conditions | 25 |
| 5 | SIMULATION METHODOLOGY | 26 |
| 5.1 | Previous Work..... | 26 |
| 5.2 | Tools & Software..... | 29 |
| 5.2.1 | Kinematics & Torque Factor Calculations Toolbox | 29 |
| 5.2.2 | Simulink/MATLAB Software | 29 |
| 5.3 | Wellbore Specifications..... | 30 |
| 5.4 | Case study 1: Conventional Unit / CSR | 30 |
| 5.5 | Case Study 2: Conventional Unit / Wire ropes | 32 |
| 5.6 | Case Study 3: Hydraulic Pumping Unit / CSR | 35 |
| 5.6.1 | Model Building | 35 |
| 5.6.2 | Blocks Configuration | 38 |
| 5.6.3 | 4-Valve Signal Commands..... | 38 |
| 5.6.4 | Polished Rod Load Implementation | 39 |
| 5.7 | Case Study 4: Hydraulic Pumping Unit / Continuous wire rope | 41 |
| 5.7.1 | Blocks Configuration | 41 |
| 5.7.2 | Signal Commands:..... | 41 |
| 5.7.3 | Polished Rod Load Simulation | 42 |
| 6 | SIMULATION RESULTS | 43 |
| 6.1 | Pumping Unit Kinematics | 43 |
| 6.2 | Hydraulic Pump Performance | 45 |
| 6.3 | Hydraulic Pump Power Consumption | 47 |
| 6.4 | Performance Comparison with Conventional Units..... | 48 |
| 7 | CONCLUSION | 53 |
| 8 | RECOMMENDATIONS..... | 54 |
| 8.1 | Wire Rope Simulation Improvements..... | 54 |
| 8.2 | Design Improvements..... | 54 |
| 8.3 | HSSE Aspects | 55 |
| 8.3.1 | Noise Protection | 55 |
| 8.3.2 | Leaks Mitigation..... | 56 |
| | REFERENCES | 57 |
| | LIST OF TABLES | 59 |
| | LIST OF FIGURES..... | 60 |
| | ABBREVIATIONS..... | 62 |

APPENDICES64

1 Introduction

Sucker rod pumps are used in the vast majority of oil and gas wells in the world. Despite being simple and easy to operate, rod pumping systems have a low energy efficiency due to the energy losses associated with the mechanical power transmission system as well as the extra power required to actuate the heavy weight counterbalance system.

In the recent years, many studies have been performed on hydraulic pumping units and the results were promising in terms of efficiency, good adaptability, light weight and energy saving. As a result, hydraulic pumping units are becoming serious competent counterparts. The main advantages of hydraulic pumping units over conventional sucker rod pumping units are: 1) The possibility to adjust and control the direction and speed of the polished rod movement by means of electrohydraulic systems, 2) The possibility to adjust the stroke length of the polished rod 3) The possibility to access critical and remote areas such as offshore fields thanks to its small footprint and light weight.

Two main goals were basically set in the beginning of this project: The first is to model a hydraulic pumping unit, analyzing its performance in terms of kinematic behavior of the polished rod (displacement and velocity curve) and compare it with the performance of conventional sucker rod pumping system when operating at the same wellbore conditions. The second is to analyze the performance of this unit when running with continuous strings and compare it with that of conventional rod string.

The work starts with an overview about artificial lift technology and sucker rod pumps in chapter 2. In chapter 3, a detailed analysis of different surface pumping units was carried out with the main focus on the different working principles as well as advantages and problems associated with each system. Having figured out all the main advantages and disadvantages of conventional beam pumps, hydraulic pumping systems are then introduced in chapter 4 as substitute artificial lift method. The analysis of different systems was performed in terms of working principle, kinematic behavior and energy efficiency. Energy saving hydraulic pumping unit was found to be the most efficient pumping system and therefore is the subject of analysis in the rest of the thesis. Moreover, the main parameter calculations and force analysis of the hydraulic pump were performed along with the calculations of the power consumption of the overall system in different operating modes. In order to analyze the performance of the suggested pumping unit, Simulink software was used for simulation considering different setups and multiple cases. Simulation details can be found in chapter 5. In chapter 6, the simulation results are presented along with the interpretations. A comparison between the suggested hydraulic unit and conventional units is performed in the end of this chapter. Finally, conclusions and recommendations are found in chapters 7 and 8 respectively.

2 Fundamentals

Over 1 million out of 2 million oil wells, worldwide, are artificially lifted. More than 750,000 of them are using sucker rod pumping systems. This chapter briefly explains the basic idea behind the use of artificial lift systems and describes the applicability of rod pumps as well as their advantages and disadvantages.

2.1 Artificial Lift Principles

Artificial lift methods are generally used to increase the production from wells when the reservoir pressure is not sufficient anymore to naturally lift the fluids to the surface. The main goal of an artificial lift system is to lower the producing bottomhole pressure (BHP) of the well in order to increase the inflow from the reservoir formation and subsequently the production rate [1]. With a wide range of artificial lift methods that can be used for this purpose, a proper selection of the most suitable lifting method is critical in terms of reliability and profitability. Therefore, the choice and design of the artificial lift system must be based on a deep understanding and analysis of the available data from previous similar cases, taking into consideration other important design criteria such as:

- Desired production rate
- Downhole flowing pressure
- Reservoir drive mechanism and pressure changes
- Oil viscosity and gravity
- Gas-liquid ratio
- Depth and wellbore size
- Wellbore trajectory
- Sand and solid production
- Scales and paraffin deposits [2]

An economical evaluation of the capital and operating costs of the system is also required in order to judge the profitability of the well.

Lowering the BHP and increasing the flow rates from an oil well can be achieved through many different artificial lift methods as mentioned before. Sucker rod pumps are the simplest and the most widely used pumping methods. They are used in 85% of the artificially lifted wells. Gas lift systems are also popular in about 10% of the wells and when properly designed they effectively achieve lower BHP and increased flow rates especially for wells with high GLRs. Progressive cavity pumps (PCPs), electrical submersible pumps (ESPs) and hydraulic pumps are also used for specific applications depending on the working environment and the aforementioned design criteria. Figure 1 shows the pumping systems distribution worldwide indicating the dominance of rod pumping methods which can be explained by the ease of usage, simplicity of the design, as well as its capability of handling moderate to very low production rates.

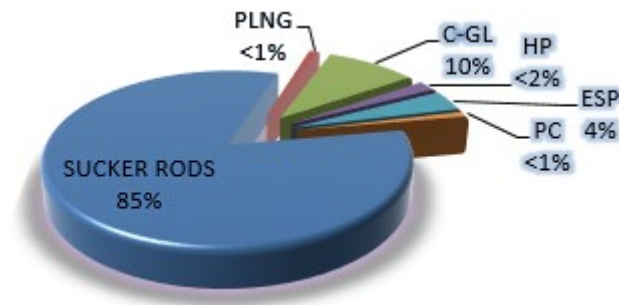


Figure 1. Usage of Artificial Lift Systems Worldwide [3]

Table 1 below presents a comparison between different artificial lift systems in terms of production capacity, operating conditions (depths, wellbore geometry, and temperature) as well as gas handling capabilities and global system efficiency.

Table 1: A Comparison between different Artificial Lift Systems [2]

| | SRP | ESP | PCP | Gas lift | Hydraulic Jet Pump |
|---|--|---|--|---|--|
| Max operating rate (BPD) | 6000 | 64,000 | 4500 | 50,000 | 20,000 |
| Max Operating Depth (TVD in ft) | 16,000 | 15,000 | 6000 | 18,000 | 15,000 |
| Fluid Gravity [$^{\circ}$API] | >8 | >10 | <40 | >15 | >8 |
| System efficiency | 45-60% | 35-60 % | 50-75 % | 10-30 % | 10-30 % |
| Gas Handling | Good if gas anchor is used, poor if > 50% free gas | Up to 40% free gas at pump suction can be handled with mixed stages | Poor if pump has to handle free gas | Excellent (reduces the amount of injection gas) | Good/fair if downhole gas separation below pump intake |
| Temperature | Excellent up to 290 C | Up to 200 C (special motors and cables) | Up to 220 C (limited due to elastomer) | Max 180-200 C | Special materials up to 260-320 C |
| Offshore Application | Poor | Good | poor | Excellent (most common method) | Good |
| Hole deviation | Typical 0 to 20 | 0-2 $^{\circ}$ max deviation of section | Poor (Wear and load problems) | Typical 0 to 50 | Typical 0 to 20 |
| Noise Level | Moderate | Very low | Low | Low (noisy at compressor) | Low |

2.2 Sucker Rod Pumps

Rod pumps are the oldest and most common form of artificial lift systems for oil wells. A typical pumping system consists basically of a prime mover, a surface pumping unit, a rod string and a downhole pump. Figure 2 shows the major components of a conventional pumping unit.

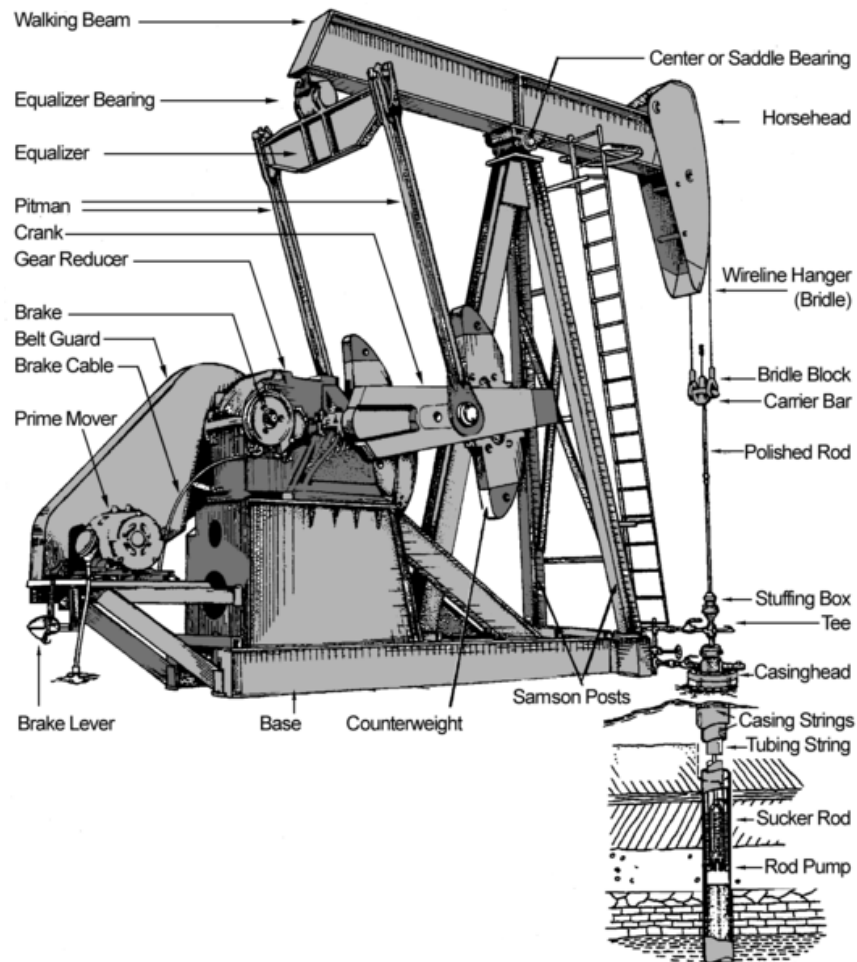


Figure 2. Schematic of Conventional Sucker Rod Pumping System [5]

2.2.1 Surface Equipment:

The rotating motion of the prime mover (motor) is converted to a vertical reciprocating movement through the gear reducer, crank and the walking beam. This motion is transferred to the downhole pump through the polished rod and the rod string allowing it to move up and down, creating the pumping action. The lifted fluids are then directed through the tubing into the surface flow line.

The prime mover is the source of power needed by the pumping unit. It could be an electric motor or an internal combustion (IC) engine. The usage of one of the two options should be based on many considerations including:

- Power source availability (electricity/ combustible fluids)
- Energy requirements
- System efficiency
- Anticipated costs (Capex, Opex, repairs...)

The gear reducer converts the high speed, low torque power delivered by the prime mover into low speed, high torque energy which is then used by the surface unit. As mentioned before, the rotational motion is converted into reciprocating vertical movement through the walking beam. Counterweights are used to balance the loads during the upstroke. The up and down

motion is transferred from the walking beam to the subsurface pump through the polished rod located at the top of the rod string and the rod string itself. The polished rod forms a tight seal with the stuffing box which is a sealing device attached to the pumping tee and used to divert the produced fluids into the flow lines. Proper materials should be selected for this device in order to avoid wear and corrosion which dramatically decrease its life span.

2.2.2 Sucker Rod String

The sucker rod string consists of individual steel rods with acceptable diameter sizes ranging from 5/8 to 1 ^{1/8} in, and typical rod length of 25 or 30 ft. These rods are screwed together to form a mechanical link that transfers the motion from the polished rod at surface to the downhole pump near the well bottom. The American Petroleum Institute (API) provides the industry with specifications and requirements of production operations. Based on their standards the main available rod grades are described below:

- Grade C: minimum tensile strength 90,000 psi, maximum tensile strength 115,000 psi.
- Grade K: The same minimum and maximum tensile strengths as grade C rods. Being made of 1.65 to 2 % nickel, they are characterized for their improved corrosion resistance, yet they are more expensive.
- Grade D: minimum tensile strength 115,000 psi, maximum tensile strength 140,000 psi.

One of the major limitations of the conventional sucker rod string is the connections between individual rods. As a matter of fact, failure statistics indicates that connection failures represents about 42% of the failure distribution along the rod string which can be explained by a lower fatigue resistance of the connections than the rod body. There are other sources of failures such as rod upset, shear coupling and rod body and they represent respectively 53%, 3% and 2% of the total failures of the sucker rod string. Figure 3 below describes the failure distribution within the sucker rod string.

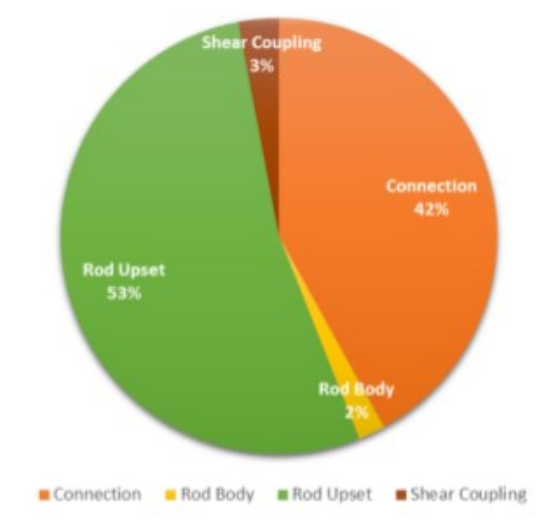


Figure 3: Failure Distribution by Location

Other concerns associated with the conventional rod strings are the long workover time spent for attaching and detaching the individual rods to form the entire string. These limitations led the industry to go for an innovative solution, for instance the substitution of the conventional rod string by a continuous string. This will eliminate the need for rod connections, resulting in the minimization of the associated failure and increasing the overall MTBF of the system.

2.2.3 Downhole Pump

The main components of the pump are: barrel, plunger, standing and travelling valve as shown in figure 4.

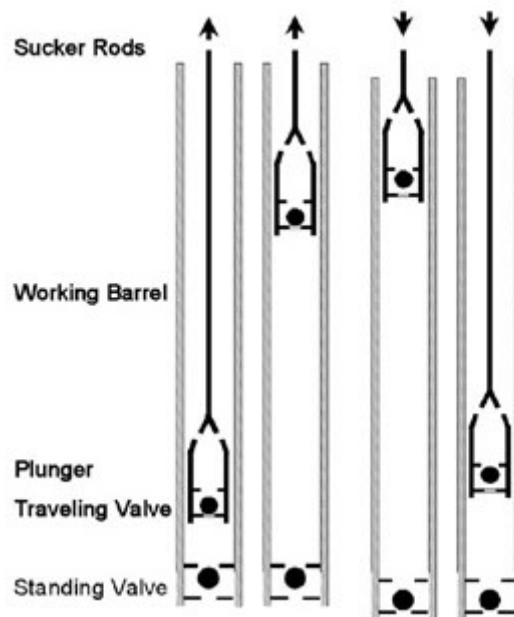


Figure 4. Full Pumping Cycle of a Downhole Rod Pump [3]

The vertical reciprocating motion of the beam is transferred through the rod string to the plunger allowing it to move upward and downward. These up and down strokes form the full pumping cycle. During the upstroke, as the plunger is pulled up at a certain velocity, the pressure inside the barrel is decreased below the pump intake pressure. Then the standing valve is open and the fluid continuously enters the barrel until the end of the upstroke when the standing valve closes. During the down stroke, the plunger travels down and the barrel pressure increases, pushing the traveling valve to open. Fluid flows from the barrel into the tubing.

Many challenges have to be faced during pump operation such as fluid pound or gas interference. These problems occur mainly due to poor design of the system or due to change in the reservoir pressure (reduction in inflow performance) after a period of time that can cause a drop in the dynamic fluid level. These problems can be detected and analyzed using dynamometer card plots (figure 5) which describe the rod tension/compression forces versus the displacement.

- a) Ideal Card: Anchored tubing, 100% liquid fillage and good pump conditions.

- b) Slanted: The card is slanted at K_{tbg} indicating that the tubing is unanchored.
- c) Fluid Pound: Sudden impact load is inefficient and damaging to the pump, rods and tubing. It causes rod buckling and rod-on-tubing slap.
- d) Gas Interference: Gradual load transfer as gas compresses. Pumping efficiency is dramatically reduced.
- e) Hole in barrel: as the plunger passes through a hole, the fluid load F_0 is lost.
- f) Worn Pump: travelling valve leaking or plunger/barrel wear.

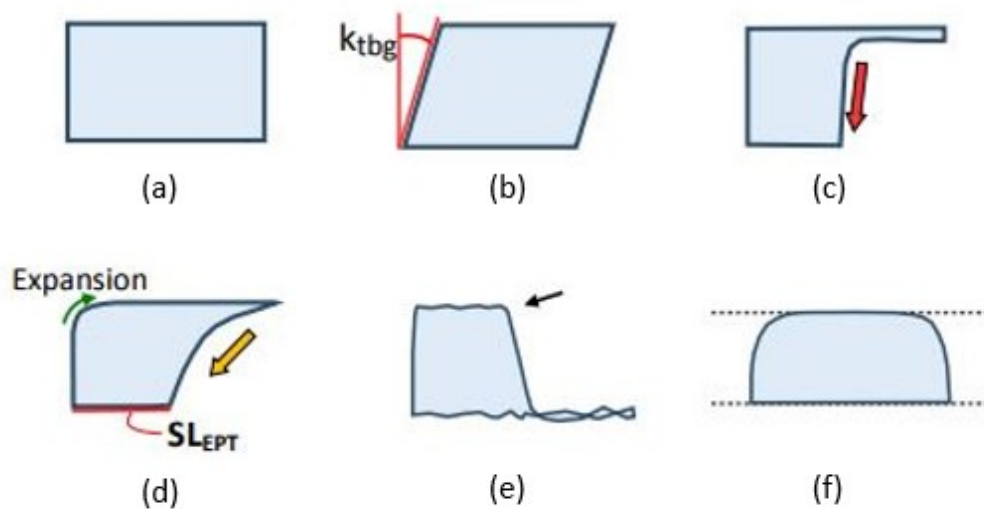


Figure 5. Pump Card Shapes Analysis [4]

Although there is a variety of available and innovative artificial lift systems, sucker rod pumps are still the first choice for most onshore and some offshore wells worldwide. Table 2 below summarizes the main advantages and limitations of sucker rod pumping.

Table 2: Advantages and Limitations of Sucker Rod Pumping System [1]

| Advantages | Limitations |
|--|--|
| <ul style="list-style-type: none"> • easy to operate • Transportation of surface unit to other wells with minimum costs • applicable for wells with low pressure/low rates • high temperature and viscous fluid can be lifted • easy corrosion and scale inhibition treatment • automation possibility | <ul style="list-style-type: none"> • need for workover operation to service downhole equipment • scales and paraffin formation • lower efficiency when installed in gassy wells (gas locking, gas interference) • crooked holes are problematic • bulky footprint (major concern for offshore) • environmental concerns regarding stuffing box leakage |

Owing to these main advantages, rod pumping systems are likely to maintain their position in the industry as the most favorable artificial lift method. The use of these pumping systems is expected to increase in the future thanks to its applicability in many unconventional areas including shale formations which require high number of wells producing at low rates. These hydraulically fractured horizontal wells are characterized by initial high pressure and high flow rates followed by a dramatic decrease in both pressures and rates making them perfect candidates to be artificially lifted by sucker rod pumps. In some cases, initial artificial lift systems that are designed for high rate wells (ESPs, continuous gas lift...) become uneconomical to use after the decline of production volumes. Therefore, the substitution of these systems by sucker rod pumps which are able to handle low volumes would be a much more economical decision. [8]

Hence, it is very important to optimize the performance of the sucker rod pumping systems in order to ensure safe and efficient pumping operations.

3 Conventional Surface Pumping Units

The chapter discusses the main structural parts of each surface pumping unit, different available unit geometries and the main problems/Limitations of beam pumping units.

3.1 Components of a Pumping Unit

As shown in figure 2, the surface unit structure is supported by a rigid steel base which is set over a concrete base to ensure the alignment of the components. The greatest load is carried by the Samson post which is designed to be the strongest component of the unit. On top of the saddle bearing -or the central rotating point- the walking beam is placed, having a large cross section to withstand the bending loads caused by the well load on one side and the driving force of the pitmans on the other side. The horsehead is located at the side of the walking beam. It has a curvature to ensure the verticality of the polished rod movement. In conventional units, the equalizer is attached to the other end of the walking beam and its role is to transmit the polished rod loads through the walking beam to the two pitmans. Counterweights are situated on both sides of the gear reducer and are driven by the slow speed crank shaft attached to the gear reducer. In a conventional unit, the counterweights are attached to the crank arm and their role is to balance the load of the produced fluid and the rod string.

The gear reducer as mentioned before, has gears to convert the prime mover high speed and low torque to low speed -desired pumping speed- and high torque needed to operate the unit. The unit is also incorporated with a brake assembly to stop it at any time. Finally, the prime mover (source of power) can be either an electric motor or an internal combustion engine.

3.2 Pumping unit's designation

The main parameters that are used to designate the pumping units are: 1) Gear reducer peak torque rating in 1000 lb-in, 2) Gear reducer type (e.g., D: double reduction gear reducer), 3) Structure number describing the maximum load on the beam (lb/100), 4) maximum stroke length in inches (distance between highest and lowest position of the horsehead).

These parameters are generally preceded by a letter describing the structural type or geometry of the unit:

- C for Crank balanced conventional unit
- B for Beam balanced conventional unit
- A for Air balanced unit
- M for Mark II unit¹
- RM for Reverse Mark unit [8]

As an example of designation: "C-456D-256-120". This unit has the following characteristics: It is a conventional crank balanced unit with a 456,000 lb-inch peak torque rating of the double

¹ Mark II and Reverse Mark are registered as trademarks of Lufkin industries

reduction gear reducer, having a 25,600 lb structure load rating and a maximum stroke length of 120 inch [9].

3.3 Beam Pumping Units geometries

All beam pumps have the same basic components; however, various arrangement types of the components result in characteristics. Depending on the saddle bearing (pivot point) location, beam pumps can be classified into two main categories: mid-beam category (class I) and end-of-beam category (class III). In the following section, the main pumping unit geometries are presented with their basic features.

3.3.1 Crank Balanced Pumping Units

Crank balanced units (figure 6) are also called conventional units. They are the oldest and most commonly used unit type. Conventional units belong to class I lever which means that the saddle bearing is located on the center of the walking beam. Because of this configuration, half of the crank's rotation (180°) is used for the upstroke and the other half is for the down stroke. As the name indicates, the counterweights are positioned on the crank arm of the unit. This unit type can be driven in both directions: clockwise (CC) and counter-clockwise (CCW).

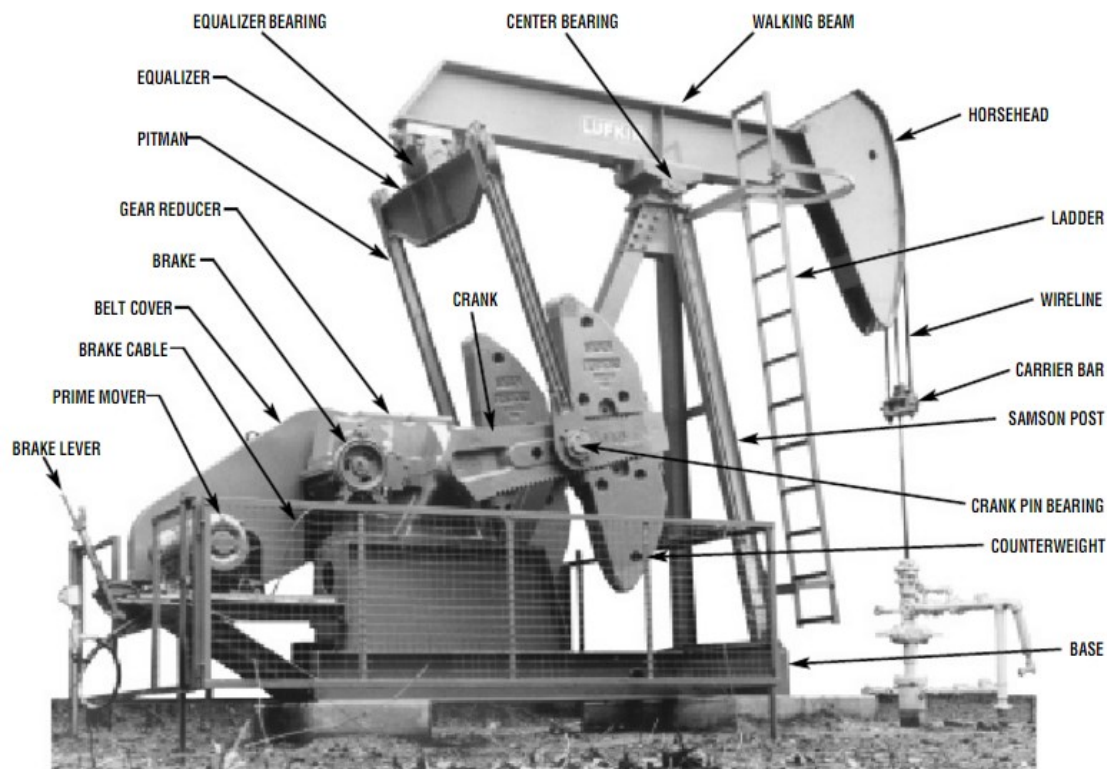


Figure 6. Main Components of Conventional Pumping Unit [14]

3.3.2 Beam-Balanced Pumping Units

The counterweights in this geometry are positioned at the end of the walking beam (Figure 7), behind the equalizer bearing. At high pumping speed, the unit is susceptible to damage. Beam-balanced units are smaller than crank-balanced units and are more attractive for shallow, low production wells.



Figure 7. Example of Beam-balanced Pumping Unit [10]

3.3.3 Air-Balanced Pumping Units

The counterbalance in this unit is ensured by the use of compressed air -as shown in figure 8- instead of counterweights. This allows for more control of the counterbalance which can be adjusted without stopping the unit. The counterbalance system includes a piston and an air cylinder, through which air is compressed to balance the load of the well. The substitution of the heavy steel counterweights dramatically reduces the weight of the unit comparably to a similar conventional unit. Therefore, this light and compact sized unit can be attractive to use in offshore platforms and other areas where the footprint of the surface facilities presents a concern.

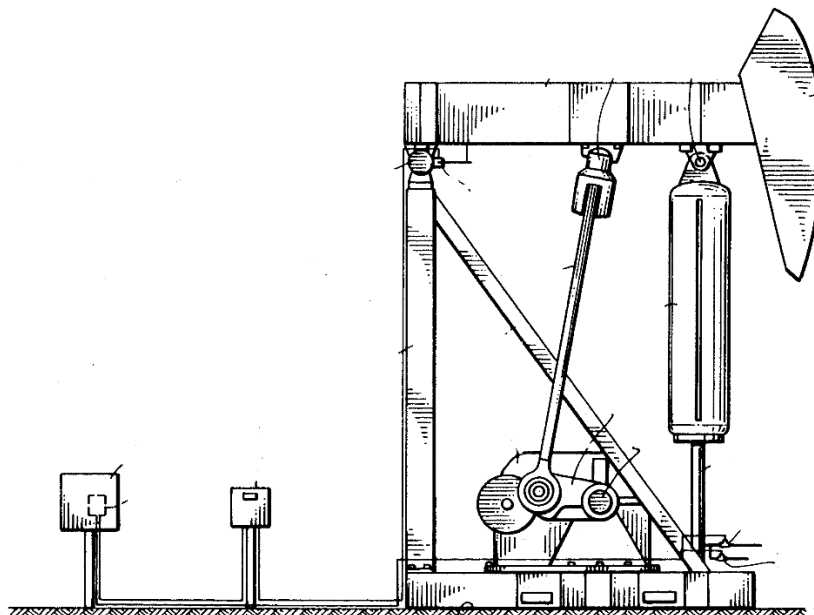


Figure 8. Schematic of Air-Balanced Beam Pumping Unit [13]

3.3.4 Mark II Pumping Units

In this configuration, the equalizer bearing is located very close to the horsehead (figure 9), this means that the upstroke uses more than the half of the crank rotation (195°) and the remaining crank rotation (165°) is used for the down stroke. As a result, the unit has a decreased acceleration at the upstroke resulting in a reduced peak polished rod load (PPRL). This is beneficial in reducing the size of the surface unit as smaller prime movers and gear reducers can be used. On the other hand, slower upstroke allows for a sufficient time for pump barrel to be filled with fluids which prevent problems of fluid pound or gas interference [1]. This results in an improved pumping efficiency. Mark II pumping unit must always be driven in counter clockwise direction.

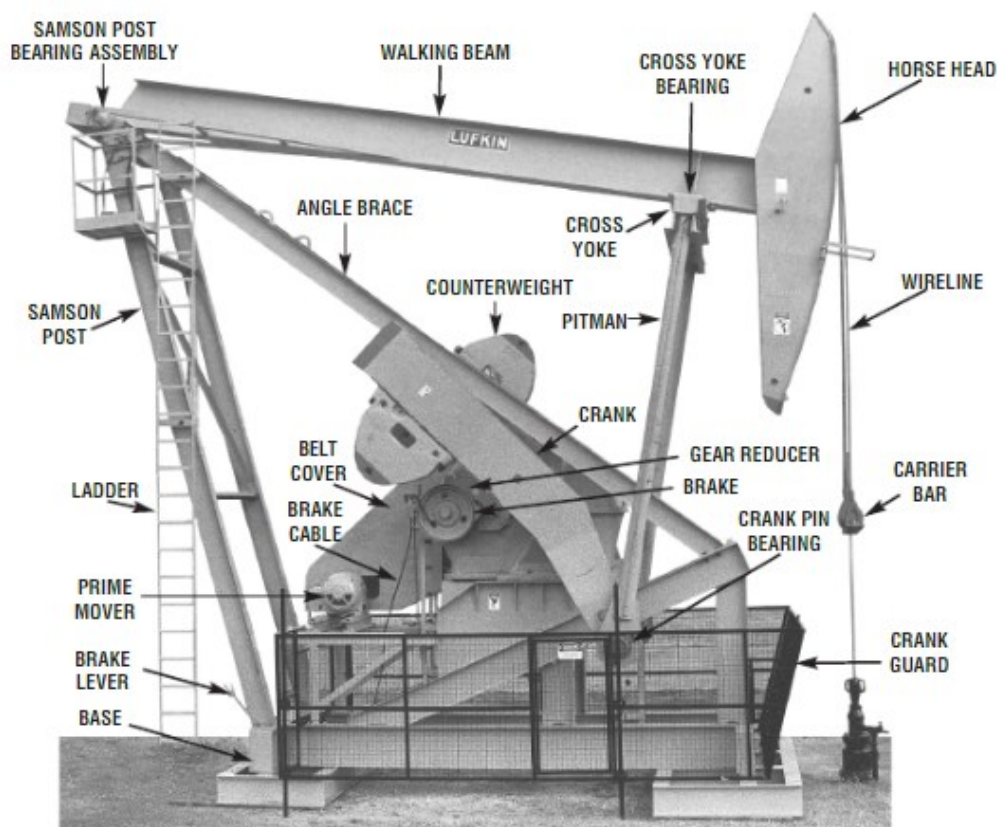


Figure 9. Main Components of Mark II Pumping Unit [15]

3.3.5 Reverse Mark (RM) Pumping Unit

This type of unit uses some features of the Mark II unit convolved with the conventional geometry. Similarly to Mark II unit, Reverse Mark unit uses phased-crank counterbalance resulting in an improved load-lifting capabilities. This geometry results in a relatively reduced peak torque compared to conventional units. Due to the phase crank, this unit must be driven only in one specific direction.

3.4 Problems with Beam Pumping Units

Rod pumping unit using a crank-driven walking beam to provide a reciprocating motion for oil and gas production have historically been and is still the most widely used artificial lift method in the petroleum industry. This pumping system is available with different geometries and

configurations in order to produce the desirable polished rod motion profile and gearbox torque loads. [10]

However, there are many problems associated with the use of these beam pumping units. One of the major limitations is that operating the unit in an efficient manner is limited to a fixed velocity profile. In other words, any change in the pumping velocity throughout the pumping cycle results in a significant amount of wasted energy which means additional operating costs. Velocity profile adjustment is done through a Variable Speed Drive (VSD), adding more capital costs to the project.

Moreover, larger units are needed when operating in deeper wells. This presents a major limitation because of the increased unit footprint especially in areas where space is a constraint. In case of well intervention, the surface unit of adjacent wells has to be dismantled expanding the lost production time. Increased weight and size is also problematic in terms of transportation, installation and workover operations. On the other hand, counterbalance constant adjustment to match the well load profile is difficult and time consuming. [11]

Any innovative solution in the rod pumping technology must take into consideration the aforementioned limitations of the beam pumping units which include: increased footprint, high energy losses, and problems with transportations and installations. Hydraulic surface pumping units have therefore been introduced to the industry as substitute to beam pumps to overcome such complications and problems. The following section presents a detailed discussion of the working principles and main features of these systems.

4 Hydraulic Surface Pumping Units

Hydraulic pump jacks are characterized by a relatively small foot print, low power consumption and few complicated equipment compared to conventional mechanically driven pumping units. Moreover, the hydraulic control of the pumping cycle allows for precise and instantaneous adjustment of the system kinematics as desired. Therefore, beam pumps have been replaced by hydraulic pumping units in many oil wells around the world aiming to improve the system efficiency and maximize the recovery factor in these fields. The results are promising from both operational and economical perspectives.

4.1 Hydraulic Pumping Unit using Gas Cylinder as Counterbalance (DynaPump)

The hydraulic surface pumping unit commercially known as “DynaPump” consists of two principal components (figure 10). The first is the hydraulic power unit that supplies the pumping unit with the required energy. The second is the pumping unit which converts the hydraulic power into mechanical force to lift the well load.

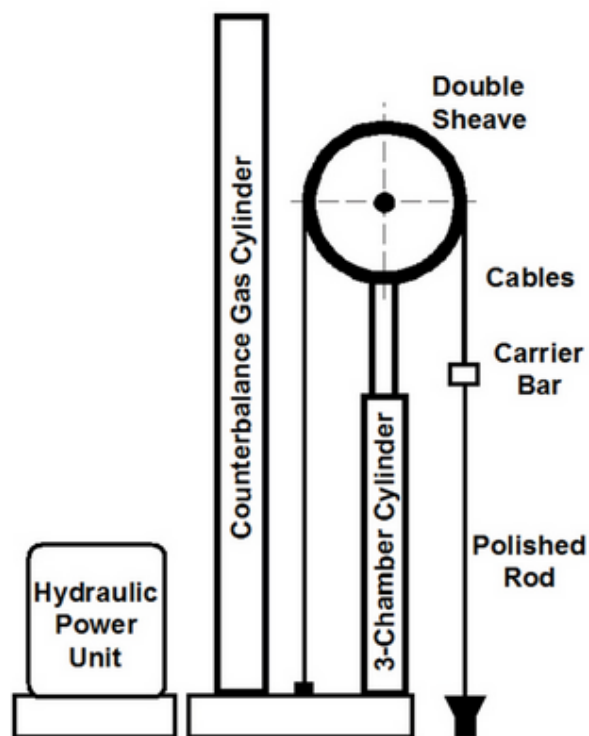


Figure 10. Structure of the DynaPump Unit [5]

4.1.1 Operating Mechanism

The pumping unit is used to drive the downhole pump through the sucker rod string. The upper end of the polished rod is attached to a carrier bar. Two wireline cables are attached at one end to this carrier bar, then run on a double sheave forming a 2:1 pulley system and finally fixed to the unit base at the other ends. As can be seen in figure 10, the sheaves are mounted on a plunger extending from a 3-chamber hydraulic cylinder. The vertical position of the sheaves can be controlled by the hydraulic flow rate received from the power unit. During the

pumping cycle, load variations are produced within the well and in order to counterbalance these loads the system uses pressurized gas (Nitrogen) which acts on the hydraulic cylinder as well. The gas cylinder on the left is used for storage purposes.

The 3-chamber hydraulic cylinder (figure 11) plays a pivotal role in the mechanism of the pumping unit as it is the heart of its mechanical operation. It is formed by three concentric cylinders two of them are stationary and the third (plunger) is moving to provide the vertical movement of the sheaves and lifts the polished rod. At the lower end of the plunger; an annular piston is connected providing seals on the inside of the outer cylinder and on the outside of the inner cylinder. This arrangement creates three different chambers as shown in figure 11 below. The pumping cycle is controlled by the power fluid and pressurized gas that are provided to the chambers in a predetermined procedure explained in this section.

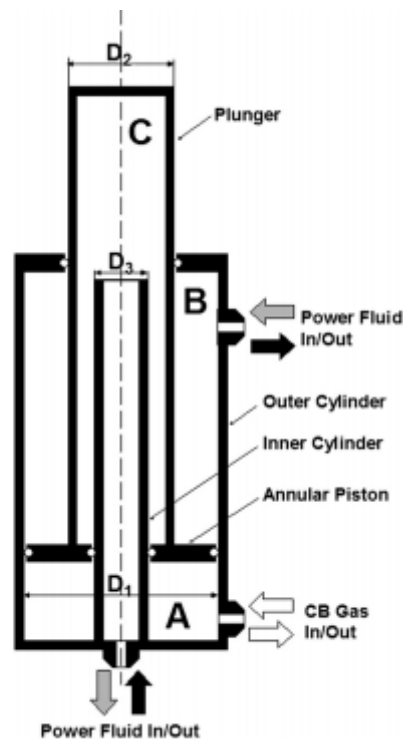


Figure 11. 3-Chamber Hydraulic Cylinder [5]

It is clear in the figure above that pressurized gas is provided to chamber A below the piston, while power fluid is connected to the chambers B and C through hydraulic valves. When power fluid is injected to chamber C (black arrow), it forces the plunger to move upward lifting the polished rod. During this upstroke, the volume of chamber B decreases leading the power fluid to exit the chamber (black arrow). It also important to mention that part of the well load is counterbalanced by the gas pressure in the chamber acting on the annular piston in the same direction of the power fluid force. This is beneficial for the system in terms of energy consumption as less force is needed from the power unit to lift the same well load. During the down stroke, the power fluid direction is reversed and it is pumped in chamber B (grey arrow). The plunger is then moving downward and gas pressure counterbalances the forces acting on the piston as well. [5]

It is important to note that the two main parameters that control the pumping cycle are the power fluid rate and direction. In fact, the flow direction affects the direction of the plunger and, in other words controls the switch of the polished rod movement from upstroke to down stroke and vice versa. On the other hand, the rate of power fluid controls the speed of the plunger. These two parameters –flow rate and direction- are controlled by a computer connected to the power unit. This is a great advantage of the hydraulic pumping unit as it offers the possibility of controlling the kinematics of the system without direct human intervention.

4.1.2 Power Unit

The role of the power unit is to control the operation of the hydraulic pump in terms of pumping speed, acceleration and deceleration of the polished rod as well as the control of the direction of the polished rod (upward/downward). Other tasks can also be performed by the power unit such as communication with external devices and control of overall system performance.

The power unit provides the pumping unit with the necessary hydraulic power. It can be driven by electric motors as well as gas engines using produced gas. It comprises also of a programmable logic controller (PLC) to control the motor driving the main pump. The power unit incorporates its own variable frequency drive as well as allowing it to change and manipulate the electrical frequencies fed to the motor driving the hydraulic pump during the pumping cycle. [5]

4.1.3 Technical Description of the Unit

Hydraulic pumping units are available with different models depending on the three chamber cylinder plunger size. Table 3 below shows a summary of the technical data of available “DynaPump” units is shown.

Table 3: Technical Data of Available DynaPump Models [16]

| Model | 5 | 7 | 9 | 11 | 13 |
|---|----------|----------|----------|-----------|-----------|
| Unit Plunger size, in | 5.00 | 7.00 | 9.0 | 11.00 | 13.00 |
| Max. Hydraulic pressure, psi | 1,800 | 1,800 | 1,800 | 1,800 | 1,800 |
| Counterbalance gas pressure, psi | 1,000 | 1,000 | 1,000 | 1,000 | 1,000 |
| Max. polished rod load, lb | 15,000 | 25,000 | 40,000 | 60,000 | 80,000 |
| Max. stroke length, in | 168 | 240 | 288 | 336 | 360 |
| Max Speed, SPM | 6.8 | 4.8 | 4.0 | 3.4 | 3.0 |
| Structural height | 23 | 28 | 34 | 39 | 41 |

The maximum polished rod load and the maximum hydraulic load are the main parameters describing the lift capacity of the unit. The maximum polished rod load related to the “model 13” is up to 80,000 lb. This presents an advantage for the hydraulic pumping unit compared to beam pumping units since this load would never be achieved by the latter. On the other hand, the maximum hydraulic pressure and the maximum counterbalance gas pressure acting on their respective piston cross section area determine the maximum hydraulic load.

4.1.4 Unit Kinematics

One of the main advantages of hydraulic units over conventional beam pumps is the possibility to control and vary most of the kinematic parameters of the system during the pumping cycle using the unit’s controller.

For better understanding of the kinematic behavior of the system it is important to analyze the drive train: VFD unit → electric motor → hydraulic pump → 3-chamber cylinder → polished rod.

We can conclude from the previous drive train that the polished rod displacement and velocity are directly controlled by the VFD. The kinematics of the pumping unit will be discussed using the polished rod kinematic parameters (position, velocity and acceleration).

During a complete pumping cycle, the polished rod velocity and acceleration pattern includes acceleration, constant velocity and deceleration for both upstroke and down stroke phases (figure 12).

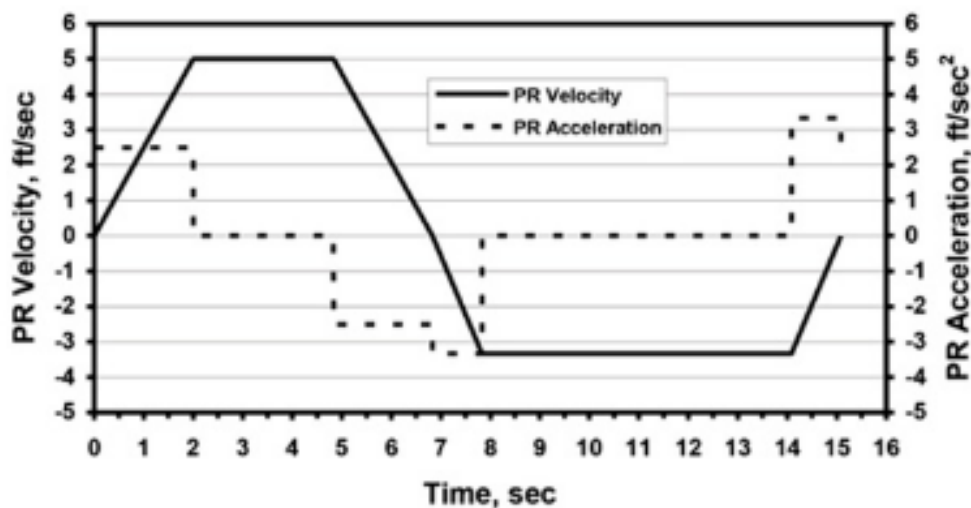


Figure 12. Velocity Profile during a Complete Pumping Cycle [5]

One important feature of the hydraulic pumping unit is that it assures constant polished rod velocities for long portions. This dramatically reduces the dynamic forces which in turn decreases the energy requirements for the system.

Another advantage is that each of the four velocities (forming a full cycle) can be independently selected resulting in an excellent unit's dynamics during the switch from one stroke to the other. [16]

The independence and flexibility in the choice of the accelerations and velocities pattern of the polished rod is a result of the relatively reduced mass of the "DynaPump" unit resulting in a very low inertia of the system. This feature improves the overall system efficiency as it results in reduced dynamic loads during the pumping cycle and dramatically lower power requirements.

4.2 Hydraulic Pumping Unit based on Electro-Hydraulic Proportional Control Technology

This type of hydraulic pumping unit incorporates an electro-hydraulic proportional control system that is able to convert the input electrical signal into hydraulic power and the rod string velocity into a feedback electrical signal to the control unit. The combination of hydraulic, electronic and automation control improves the system efficiency in terms of fast instantaneous response, high output power and high control precision. As a result, the control of the fluid flow direction and rate can be easily done by controlling the polarity and amplitude of the input electrical signal.

4.2.1 Hydraulic System Design

The main components of the hydraulic control system of the hydraulic pumping unit are shown in figure 13.

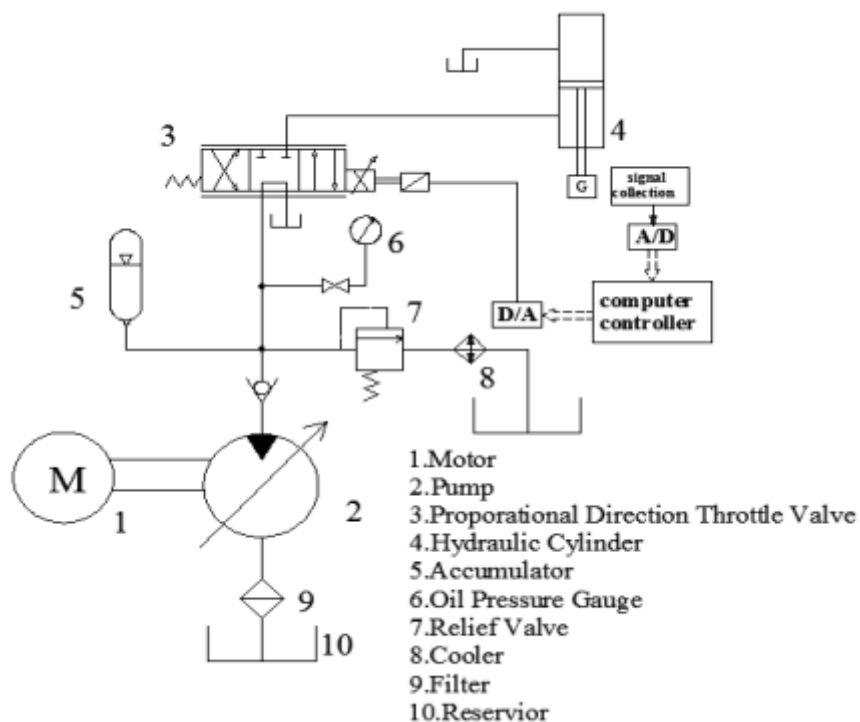


Figure 13. Hydraulic System of Hydraulic Pumping Unit

The motor drives a positive displacement pump that pumps the hydraulic fluid to the proportional valve. The control fluid flow direction and rate are regulated by the proportional valve based on the feedback signals which are proportional to the dynamic behavior of the rod string.

The speed sensor shown in the diagram (figure 14) is a linear variable differential transformer (LVDT). The speed signal is detected and converted to a digital signal through the A/D module. The digital signal is processed by the computer controller (CPU) and converted again to an analog signal by means of a D/A module. Finally, this analog signal is fed to the proportional valve and based on it the throttle size and direction of the ports are adjusted.

The pumping cycle starts when the hydraulic fluid is directed by the proportional throttle valve to the bottom of the hydraulic cylinder. The fluid acts on the bottom of the rod piston to lift it upward. The sucker rod string which is connected to the bottom of the piston is then raised with the same speed and direction. On the down stroke phase, the weight of the sucker rod string forces the piston rod to move downward. The control fluid beneath the piston is then directed through the valve to a reservoir.

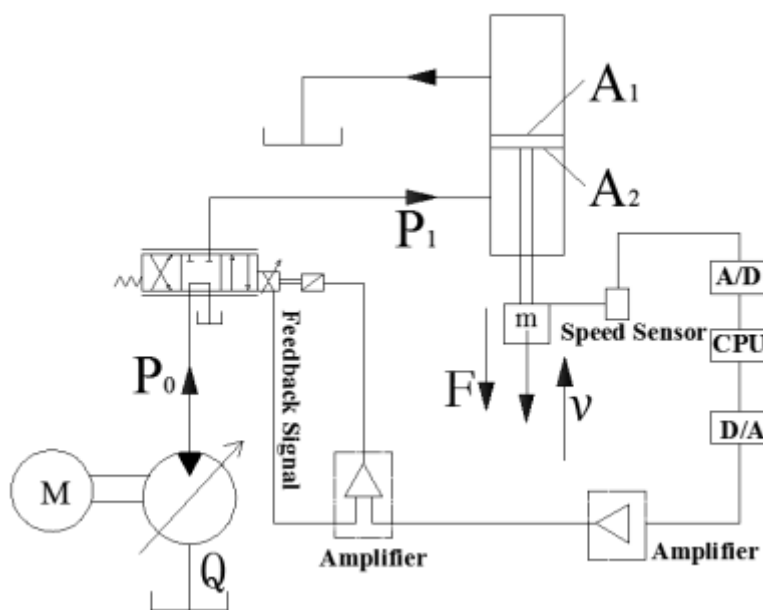


Figure 14. Hydraulic Control System of the Hydraulic Pumping Unit [17]

4.2.2 Speed Curve Design

The hydraulic pump has a speed curve with a trapezoidal shape (figure 15) which is different from the harmonic motion of the conventional beam pumping unit.

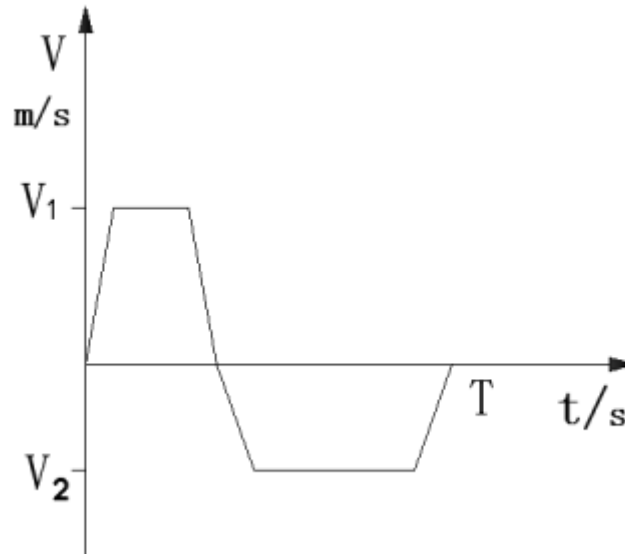


Figure 15. Speed Curve of the Pump [17]

A full pumping cycle can be summarized by describing the speed variation of the rod string which is as follows: an initial acceleration followed by a constant speed section and finally a deceleration phase. This cycle is repeated alternatively to form an upstroke and a down stroke motion.

It is clear that the up stroke and down stroke phases in the speed curve are not symmetrical. In effect, the upstroke phase is relatively faster ($V_1 > V_2$) therefore the oil leakage during this phase is minimized. On the other hand, the slow down stroke allows for maximum oil absorption and dynamic liquid level elevation.

4.3 Energy-Saving Hydraulic Pumping Unit (HPU)

The previously discussed hydraulic pumping units have relatively high energy losses due to the use of the hydraulic accumulators. An accumulator is a hydraulic device that recovers and stores energy during the down stroke phase in the form of fluid pressure. This potential energy is then released in the form of mechanical force to balance the well load during the upstroke phase. This repetitive conversion of energy from mechanical to potential form (fluid pressure) and vice versa results in additional energy losses and therefore higher capital costs due to the additional components needed for energy conversion. Although the energy loss is less than that of a conventional unit, yet it results in relatively high power requirements.

In order to overcome the drawbacks of the aforementioned pumping systems, a novel energy-saving HPU was proposed. This unit is used to operate two symmetrical oil wells simultaneously in a way that the weights of their sucker rods will balance each other. This novel design allows for continuous oil pumping from the two alternating wells as well as power saving.

Another important feature of this HPU system is that it can run a single well in case that the second needs maintenance.

4.3.1 Energy-Saving HPU Working Principle

As seen in figure 16, the 2-chambers hydraulic cylinder is installed between the two alternating oil wells. Starting by activating the directional valve at its left position, control fluid is directed to the left chamber of the cylinder. The piston rod is then pushed to right and lifts the left sucker rod string by means of the pulleys system. Meanwhile, the right sucker rod string performs its down stroke and assists with its potential energy the load balance of the left side well. In order to control the pumping speed of the system, a proportional valve is used with a programmable input signal. When the piston rod reaches its maximum right position, the directional valve switches the working position to the right side. Hydraulic oil is then directed to the right chamber pushing the rod piston to the left side and the same process previously discussed is reversed.

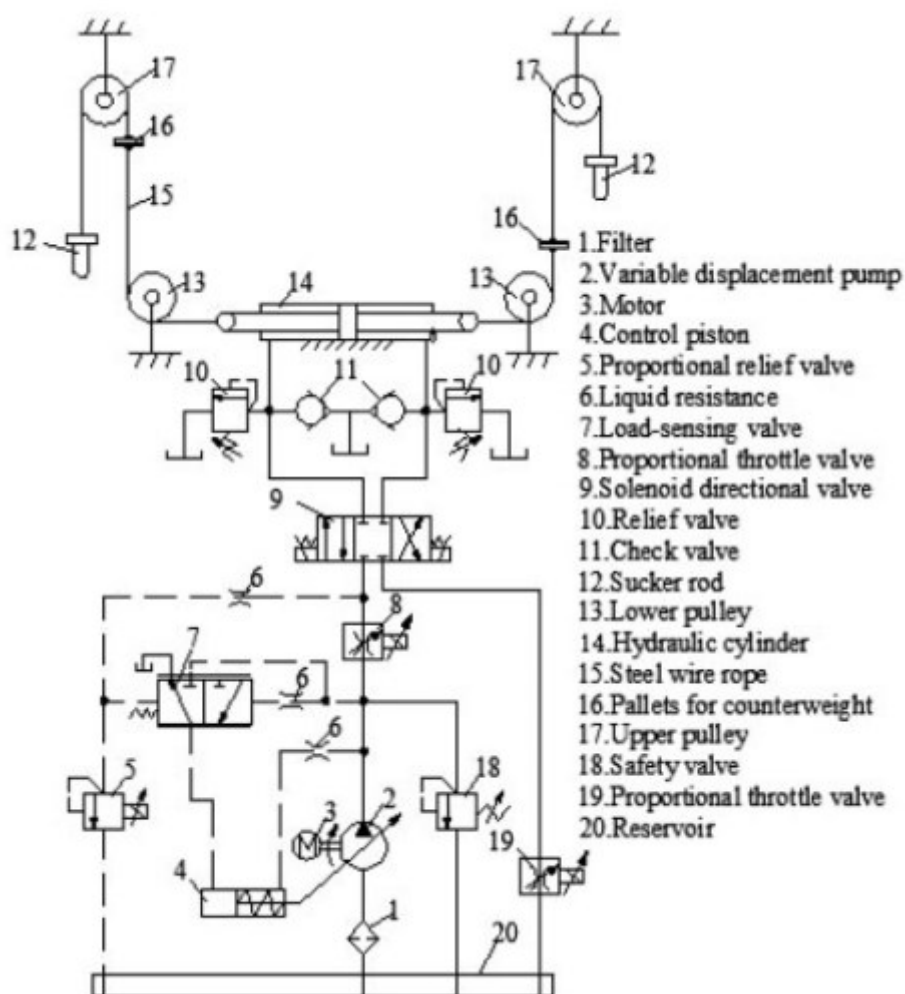


Figure 16. Working Principle of the Energy-Saving HPU [18]

As mentioned before, this system allows for a single well operation if one of the wells needs maintenance. This is simply achieved by removing the steel cable from the side of the non-producing well, and installing the counterweights between the two pallets. The pumping process remains the same as described.

4.3.2 Speed Curve Design

The velocity profile shown in figure 17 is obtained based on field data and actual operating conditions. Similarly, to previous HPUs, the speed curve is designed to be trapezoidal. The pumping cycle starts with an acceleration phase that lasts 1 second according to figure 15 then a constant speed phase and finally a deceleration phase lasting 1 second as well. The stroke length of this unit is 3 m and a full pumping cycle takes 12 seconds in total.

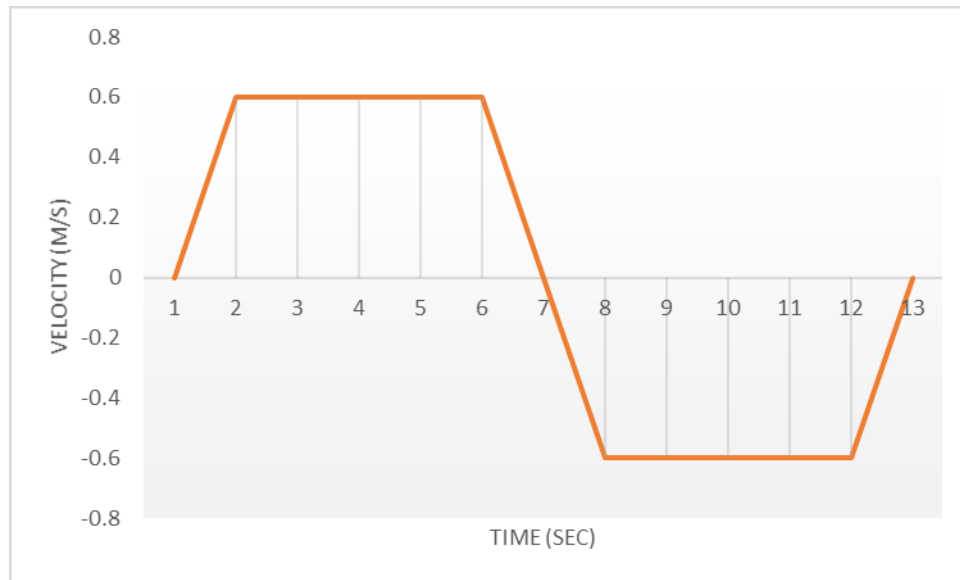


Figure 17. Energy-Saving HPU Speed Curve Design [18]

The trapezoidal velocity profile has a great advantage over the harmonic sinusoidal profile in terms of maximum speed value and as a result in terms of flow rate and power requirements. To simplify this idea, a quick example is presented below:

In this example, a sinusoidal profile is applied on the pumping unit instead of the trapezoidal one. Sinusoidal wave is mathematically represented using formula (1):

$$V = A * \sin(\theta t) \quad (1)$$

The pumping speed is 5 SPM and the stroke length is 6 m. Using formula (1), $A=1.57$ and $\theta = 6$ m. therefore, $V_{\max} = 1.57$ m/s

However, for the trapezoidal profile, $V_{\max}=0.67$ m/s. It is equal to 70% of the maximum velocity in the sinusoidal curve.

In better words, using trapezoidal velocity curve, the polished rod needs 30% less velocity than the harmonic sinusoidal velocity profile to achieve the same stroke length with the same SPM. As a result, the hydraulic flow rate requirements are less and the savings in power consumption are obvious.

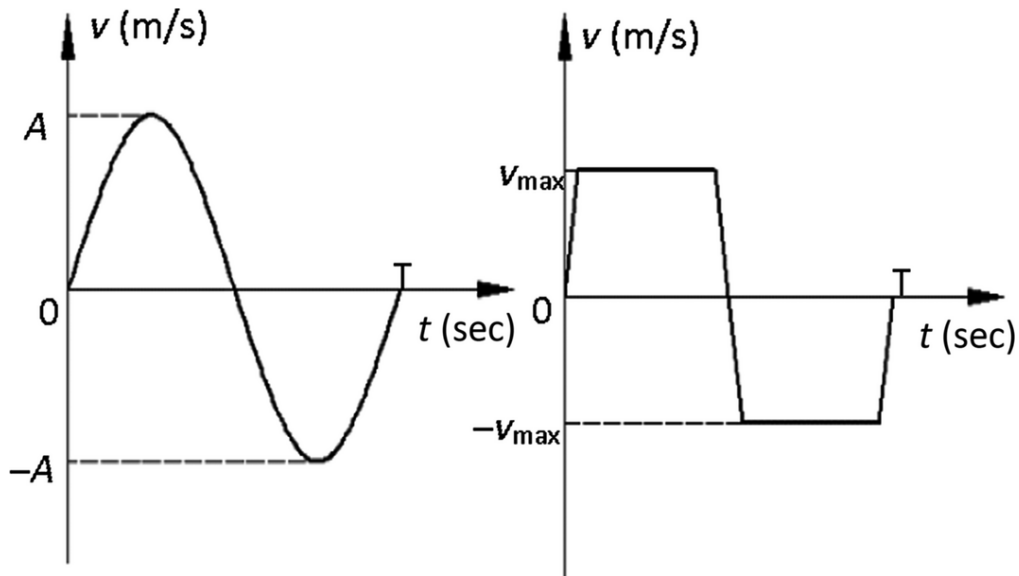


Figure 18: Comparison between Sinusoidal and Trapezoidal Velocity Curves

4.3.3 Parameter Analysis and Calculations of the Hydraulic Unit

Author Zhenhe Li came up with a mathematical definition and the primary design of the main working parameters that are referred to later on for the simulation of the pumping unit. These parameters include: the design of the speed curve (in terms of velocities and accelerations), force analysis of the hydraulic cylinder, parameter calculations of the hydraulic system (Pressures and flowrates mainly) as well as the calculation of the power consumption of the overall system.

The Following section briefly describes the methodology of the force analysis that were performed for both operating modes of the HPU: double-well and single-well operating mode.

The primary parameters that were the base for the calculations were not calculated but directly obtained from the field data as they vary from one well to another. These parameters are: Peak polished rod load (PPRL), maximum working stroke and the working period.

Starting with the design of the velocity profile, the maximum speed and the specific period for each phase (acceleration, constant and deceleration phase) can be derived from the speed curve (figure 17) and then used to calculate the polished rod acceleration. The next step is the analysis of the forces that are acting on the hydraulic cylinder.

Figure 19 below shows a double acting cylinder with a rod extending from both ends where the polished rods of the two alternating oil wells will be connected as discussed before.

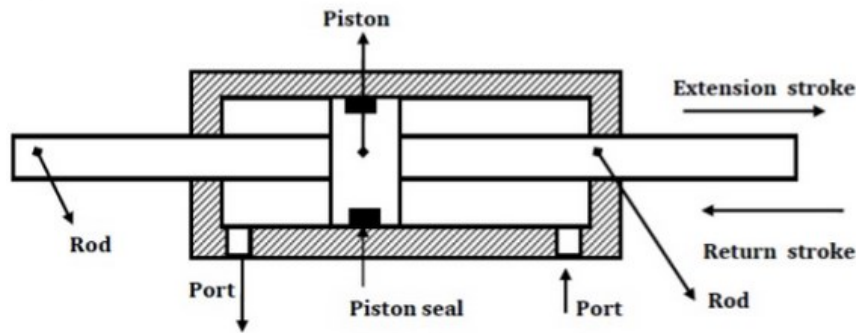


Figure 19: Double Acting Hydraulic Cylinder with Piston Rod [27]

This hydraulic cylinder has a port at each end in order to be supplied with working fluid acting alternately on both sides of the piston. Thus, the extension and retraction of the piston is achieved allowing for the up and down stroke of the attached rod string.

The main role of the hydraulic cylinder is to create a lifting force that overcomes the well loads, therefore it is important to analyse all driving forces required by the sucker rod.

The main forces that contribute during the pumping operation are: inertial force of the sucker rod, the resistance of overcoming seals, friction between the steel wire rope and the upper and lower pulley [18].

The resultant force that is acting on the hydraulic cylinder is not only dependent on the mentioned forces coming from well loads and friction but also on the different operating modes of the pumping system. In fact, changing the operating mode of the pumping system from double-well operating mode to single-well operating mode will result in a considerable change in the resultant force, which in turn affects the design of the components of the hydraulic system as well as the power requirements of the hydraulic pump.

Another important factor that highly affects the force calculation of the hydraulic cylinder is the movement regime of the rod string/ piston rod. More precisely, the largest driving force required by the sucker rod is observed in the acceleration phase, which is absolutely different from the resultant force during the constant velocity phase where inertial forces are neglected. These inertia effects will be clearly seen later in the simulation results as they are affecting the power consumption curve of the hydraulic pump.

A simplistic methodology to analyse and calculate the predefined forces can be seen in the flow diagram in Appendix A. In this chart, all the discussed constraints and conditions are included in order to cover all possible cases that might be faced during the pumping operation.

A detailed analysis and checking of each of the calculated forces is extremely important because the obtained force is the base of the whole following work which exists in the calculation of the parameters of the hydraulic system such as the effective working area of the hydraulic cylinder, piston diameters, actual working pressure of the hydraulic pump...etc.

In order to ensure effective working performance of the pumping system, each component of the hydraulic circuit should be properly designed and sized in dependence to the total force and associated pressure exerted by the well side.

The calculation steps of the hydraulic unit parameters are briefly described through the flow chart that can be found in Appendix A as well.

The hydraulic pump should be designed in a way to supply the hydraulic cylinder with the necessary flow rate of working fluid in order to displace the piston and perform the stroke.

4.3.4 Power Consumption under single Well Operation Conditions

As mentioned before, this type of pumping system offers the opportunity to operate a single well independently when the other does not work properly and needs workover.

In the single well operation conditions, the overall mass of the moving rod string does not change because of the implementation of the counterweights. Therefore, the inertial forces are equal to those under double well operating conditions. The seal resistance of the piston rod stays also unchangeable in this case. The unique forces that change when moving from double to single well operating conditions are the friction forces between the wire rope and the pulleys and they become half since the two pulleys associated with the second well won't be considered.

The force analysis and power consumption calculations for this setup are performed following the same procedure used already for the double well operating conditions and are also mentioned in the flow charts in Appendix A.

5 Simulation Methodology

The main focus of this project is the technology of hydraulic pumping systems as they have shown great performance in terms of energy efficiency and system control when implemented in oil wells instead of conventional rod pumping systems.

Another motivating factor for the design of this unit is that previous studies have been working on continuous wire ropes as substitute to conventional rod string and the results were promising in terms of increase in the mean time between failure (MTBF), productivity as well as energy efficiency [20]. However, implementing these continuous wire ropes with conventional sucker rod pumping units posed some adaptability problems because of the lack of control in the stroke length resulting in string stretches, which in turn reduced the overall production efficiency of the system.

Hydraulic pumping systems have different designs and working principles, which are covered in the literature review part. In the following section, inspired by all presented technologies, a hydraulic pumping unit was designed for further investigation and analysis as it is believed to be the most promising pumping unit.

The suggested unit will be simulated using Simulink® software to analyze its performance in terms of motion and speed control of the polished rod/ sucker rod string as well as power requirements. Further on, the unit should be tested for its applicability with continuous rod strings. Hence the Simulation and analysis of the new pumping unit does not only consider conventional rod string but also wire rope, as well as offering a detailed performance comparison.

In order to highlight the benefit of this innovative pumping technology, four case studies are presented in this chapter including:

- 1) Conventional unit / Conventional sucker rod string (CSR)
- 2) Conventional unit / Wire rope string
- 3) Hydraulic Unit / Conventional sucker rod string
- 4) Hydraulic Unit / Wire rope String

The model setup as well as the main parameter configurations for each of the mentioned case studies are covered in the following section.

5.1 Previous Work

As described already in the literature, sucker rod string is one of the main components of the sucker rod pumping system and it is used to transfer the reciprocating movement from the surface polished rod to the downhole pump. This component represents a weak point in this artificial lift system, as it is the source of several failures such as damaging rods, unscrewed couplings as well as time-consuming procedures of attachment/detachment and transport of the rods. [20]

The Analysis and Simulation of the performance of Continuous wire ropes using a prototype software developed in Abaqus was performed in 2016 at the Chair of Petroleum and

Geothermal Energy Recovery at Montanuniversität Leoben as part of the Master thesis of Mrs. Fatemeh Fazeli Tehrani, Dipl.-ing. [20]. This novel idea will allow the operators to avoid failures that are associated with traditional rod strings by dispensing with rod couplings and reducing loads on the surface pump jack. [20]

The novel software was part of the Doctoral thesis of Dr. Clemens Langbauer, performed in 2015 at the chair of Petroleum and Geothermal Energy Recovery at Montanuniversität Leoben [25].

According to the results, replacing the CSR with continuous wire ropes has many advantages such as lighter string weight resulting in lower energy requirements, higher adaptability to small footprint long-stroke units, increased Tensile strength and increased MTBF. [20]

The simulation results of the aforementioned work are also of great importance as they are the basic input parameters of the simulation of the proposed pumping unit. Therefore, explaining the previous simulation workflow will help understanding the rest of the simulation process of the suggested unit.

The simulation process can be summarized into 5 steps: the first step is the preparation of a MATLAB file in which the string components are defined using elements and nodes along with other important parameters such as Cartesian coordinates of the nodes, Measured Depth at each node and fluid friction at each node... etc. An Abaqus element analysis so called B32 is used to collect nodes to elements. It consists of 3 nodes and 2 integration points at which stresses are observed. Further on, a MATLAB code is generated, in which the boundary conditions are specified. Several datasets need to be inserted in this code such as SPM, rod string diameter and pump size... etc. Along with these datasets, further calculated data for fluid friction of the string are inserted in another file. All these data represent part of the input file required by the developed Abaqus program. The 3rd step consists in defining the installation modes. In this simulation, two options were basically considered: the first is the standard installation in which the sucker rod string is attached from the top to the polished rod and from the bottom to the pump plunger and is free to move along the tubing string. The second installation mode considers an innovative technology called 'SRABS' (Sucker Rod Anti-Buckling System) [25].

The aim of this technology is to reduce buckling effect by extending the rod string beyond the pump barrel and exiting at the bottom. This will eliminate the buoyancy effect of the liquid column in the tubing on the bottom of the string and replaces it by the liquid load in the annulus, resulting in a dramatic decrease in the total buoyancy forces. Generally, a tensioning element such as a heavy weight can be implemented below the pump to pull down the whole string and keep it in tension.

A simplistic illustration of the SRABS mechanism is shown in figure 20.

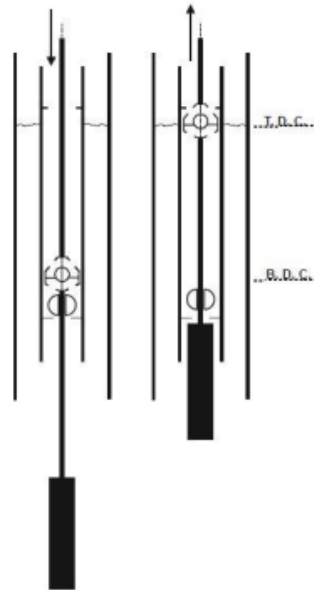


Figure 20: SRABS Pump Mechanism with a Weight

The model installation can be configured during the simulation process by adjusting the load calculation during the down-stroke phase in the MATLAB file depending on the desired setup.

After defining all elements and boundary conditions into input files, the 4th step, which is the main Abaqus code, takes place and other physical properties are inserted such as Poisson ratio, diameter of the string and modulus of elasticity. Further on, different cases are considered in terms of friction factors between string/tubing and protector/tubing along with clearances and placed in the code. The elastic behavior of the material should be also defined precisely. Furthermore, the pumping speed of the unit is defined and expressed in SPM (Strokes per Minutes) depending on the model installation. In effect, as discussed in the case of SRABS pump, the barrel volume is reduced by the extending rod beyond it. As a result, a faster pumping speed should be considered when operating with such model installation in order to equalize the production rates with the case of standard installation mode.

Finally, output files are created in which all the important results such as contact forces, stresses and movements can be found and analyzed. These parameters data are gathered through a Python program and an information folder is generated. 3 extra files are also created by the python code, explaining the time increments, reaction force at polished rod and displacement at the plunger. [20]

It is important to note that, the polished rod stress vs. time data are collected out of these results and used later on as input data for the analysis of the different case studies. Before being implemented to the simulation models, the data should be treated and reorganized in order to be adaptable to the simulation software and tools of this work. The data treatment and implementation process are explained in details in the simulation methodology chapter.

5.2 Tools & Software

In this work, two main categories of sucker rod pumping systems were modeled and analyzed. The first is the conventional unit which was modeled using an excel calculation toolbox. The second is the proposed hydraulic unit and was modeled using Simulink/MATLAB Software.

The description of the tools and their working principles can be found in the next chapters.

5.2.1 Kinematics & Torque Factor Calculations Toolbox

This tool was developed and published at the University of Texas, Austin [22], and it consists of an excel spreadsheet in which a calculation model is specifically created for the calculation and analysis of several aspects of the conventional sucker rod pumping system such as kinematic behavior, torque factors calculations and dynamometer card interpretation.

As it is shown in Appendix B, the excel model allows for inserting the pump specifications along with other important parameters such as pumping speed (SPM) and direction of the crank rotation. The polished rod position, velocity and acceleration are then computed for each 5 degrees of crank rotation and then plotted as figure 21 shows.

Moreover, by inserting the polished rod load data at every 5 degrees of crank rotation and the effective counterbalance at 90 degrees, the polished rod load curve is plotted along its position as well as the Gearbox torque versus the crank angle.

5.2.2 Simulink/MATLAB Software

Simulink is part of Matlab software developed by the MathWorks. It is a commercial tool for modelling, simulating and analyzing dynamic systems. Its primary interface is a graphical block diagramming tool and a customizable set of block libraries such as control system blockset, mechanical blockset, hydraulic blockset and many others. [19]

Creating a simulation model using Simulink consists of connecting different blocks together. Each of the blocks should be properly configured in order to meet the associated role. Once the model is built and configured, it can then be simulated in discrete or continuous sample time by Simulink engine.

One of the useful toolbox that are available in Simulink library is Simscape fluids (also called SimHydraulics®). In this toolbox, a set of component libraries are available for modelling and simulating hydraulic systems. The hydraulic circuit of the proposed pumping unit was built using the components that are available in these libraries such as hydraulic pumps, actuators, valves and pipelines...etc. [23]

Simscape allows for developing control models and parametrizing these systems using several MATLAB variables and expressions.

After simulating the model, Simscape offers different tools allowing visualization of simulation output such as charts.

5.3 Wellbore Specifications

In order to simplify the comparison between the simulation results from different case studies, the simulated models are considering the same well conditions. The wellbore information and fluid properties are enclosed in the table 4 below:

Table 4: Wellbore Specifications

| Specifications | Unit | Value |
|-----------------------------|-------------------|-------|
| TVD | m | 877 |
| MD | m | 893 |
| Temperature | °C | 61 |
| R_s | - | 0.45 |
| WC | % | 98 |
| Fluid density | kg/m ³ | 905 |
| Tubing ID | in | 2.995 |
| Tubing head pressure | bar | 5 |
| Casing head pressure | bar | 4 |
| Dynamic fluid level | m | 456 |

5.4 Case study 1: Conventional Unit / CSR

The case study of a conventional pump jack with conventional string is included within this work as a base case with which results from the next case studies, more specifically: the two case studies related to the hydraulic unit, will be compared in order to observe the advantages and main features of the new pump design.

The pump jack that has been already used in the previous work described in section 5.1 is used in this case study and therefore its specifications, in table 5 below, were implemented in the kinematic calculations model explained in section 5.2.1.

Table 5: Pump jack Specifications

| | | |
|-----------------|---------------|--------|
| Unit: | C320D-256-144 | |
| Gear Box | 320000 | in-lbf |
| Beam | 25600 | lbf |

As it can be seen in the Appendix B, operating with 5 SPM pumping speed, the position, velocity and acceleration of the polished rod were calculated for each crank angle (figure 21) (from 0 to 360° with 5° step).

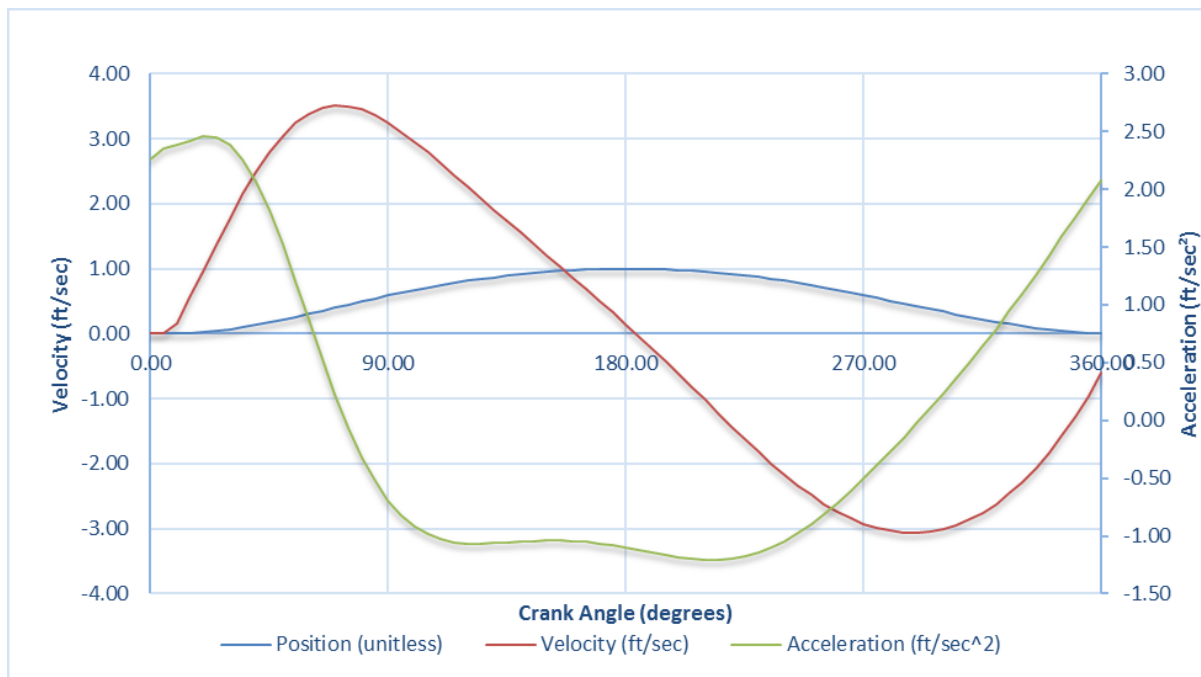


Figure 21: Polished Rod Motion - Conventional Unit / CSR

One of the most important steps is converting the stress data of the polished rod, obtained from the Abaqus simulation results that are already explained in section 5.1, into load data that can be implemented into the excel toolbox in order to visualize the dynamometer card of the pumping unit. The conversion process is described through the flow chart shown in Appendix C and can be summarized as follows:

The primary data obtained from the Abaqus simulation results related to the standard case, which is conventional sucker rod pump operating with CSR, represent the polished rod stress recorded over time as the pump was operating with 5 SPM. The dataset begins with 3 seconds of static conditions and therefore, the actual stroke is considered after this period and lasts 12 seconds. Considering 1-inch cross section area of the polished rod, the load data are then derived over the simulation time out of the stress data.

At this stage, polished rod load data were obtained over the simulation time, which is 12 seconds (without considering the static condition). However, the load data that must be implemented in the excel model, need to correspond to the crank angle rotation with a step of 5 degrees. This challenge is tackled as follows: as seen in figure 21, the position and velocity of the polished rod are calculated over the crank angle rotation. As a result, a new time axis can be derived which in turn corresponds to the crank angle rotation. In simpler words, each point in the new time axis corresponds to 5 degrees' rotation of the crank angle.

The next step is to interpolate the polished rod load data recorded over the simulation time in order to obtain the load data that correspond to the newly derived time axis. Finally, the polished rod load is obtained for every 5 degrees rotation of the crank angle and can be then successfully implemented in the described excel toolbox.

In order to visualize the dynamometer card of the pumping unit, the load data are plotted over the polished rod displacement and the results are shown in figure 22.



Figure 22: Dynamometer Card – Conventional Unit / CSR

5.5 Case Study 2: Conventional Unit / Wire ropes

In this case study, the same conventional unit was running with continuous rope instead of CSR. The downhole pump setup was changed as the SRABS pump (described in section 5.1) was installed, and therefore the pumping speed was slightly increased from 5 to 6 SPM in order to equalize the productivity of the pump with the previous case study. Polished rod data were obtained from Abaqus simulation and implemented to the excel calculation toolbox following the same procedure for case study 1.

Table 6 below describes the main characteristics of the wire rope in comparison to a CSR.

Table 6: Design Specifications of CSR string and Wire Rope

| Material | Composition | diameter | Density | Weight per Length | Elongation at break | Modulus of Elasticity | Tensile strength | Poisson Ratio | Temperature Limit |
|------------------------|-------------|----------|-------------------|-------------------|---------------------|-----------------------|------------------|---------------|-------------------|
| (unit) | - | mm | g/cm ³ | Kg/100m | % | GPa | GPa | - | °C |
| Conventional SR | Steel | 15.9 | 7.85 | 250 | 4.17 | 192 | 0.8 | 0.3 | - |
| Wire Rope(Voestalpine) | Steel | 13.6 | 7.81 | 114.2 | 0.99 | 187 | 1.8 | 0.3 | - |

From the design point of view, continuous ropes (CR) are characterized by a relatively lower weight resulting in smaller counterweight requirements and lower energy consumption [20].

The position, velocity and acceleration of the polished rod were also plotted for this case study as shown in figure 23

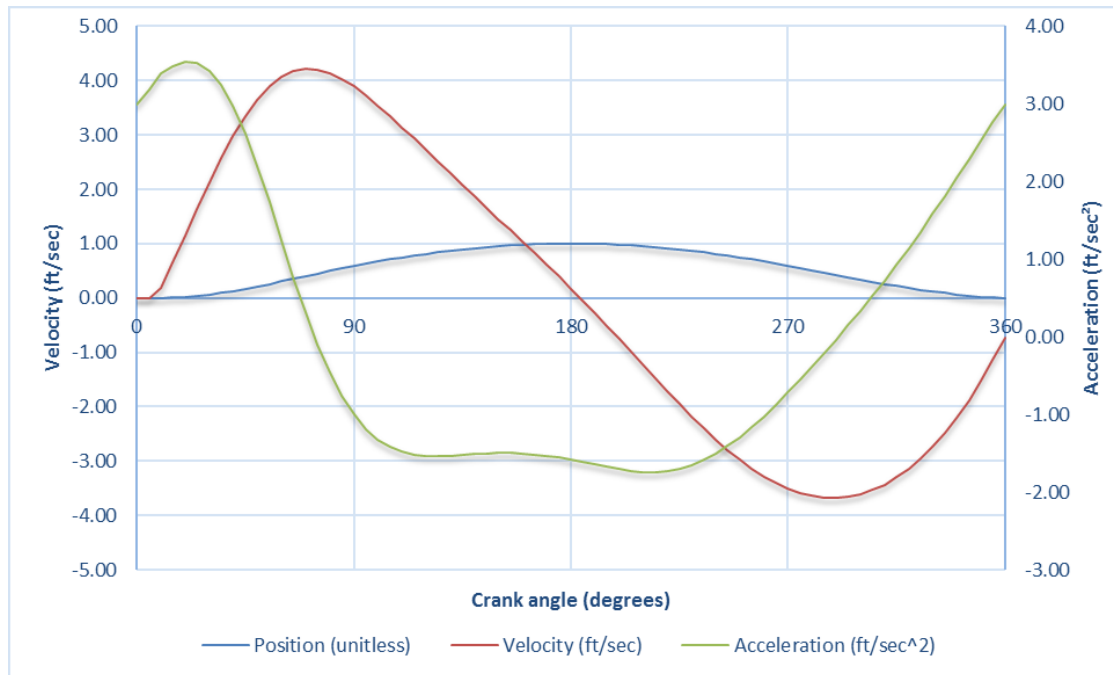


Figure 23: Polished Rod Motion - Conventional Unit / Wire Rope

Following the same procedure for the case of CSR, the polished rod load curve for the conventional unit with continuous wire ropes was also constructed and shown in figure 24.

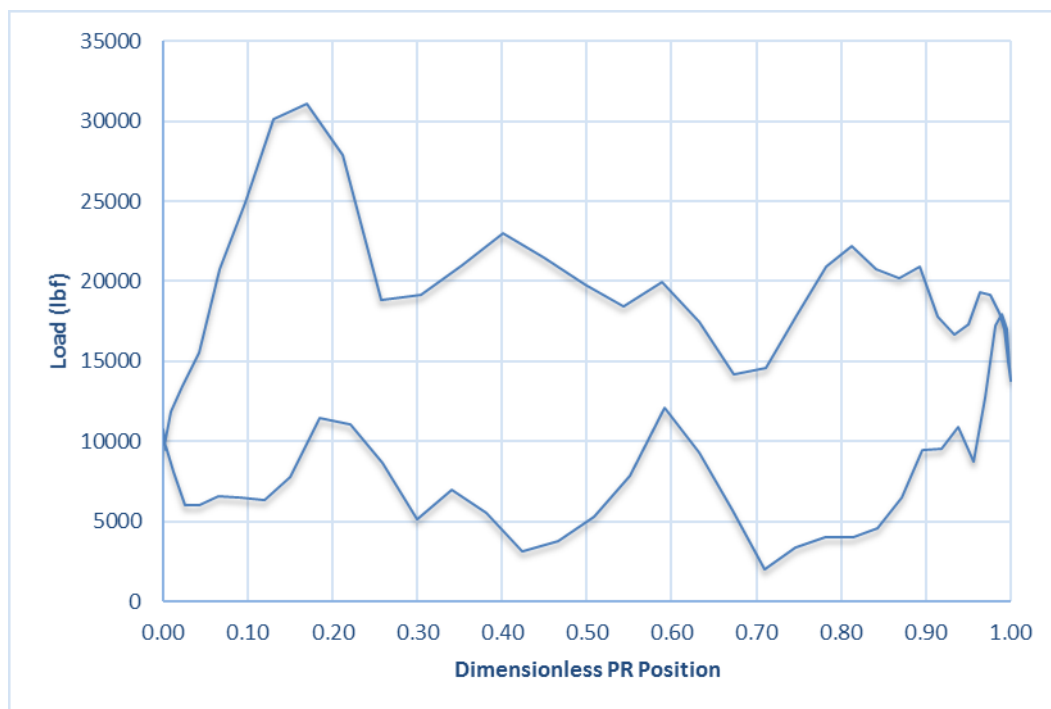


Figure 24: Dynamometer Card - Conventional Unit / WR

Despite all advantages that the wire rope string brings, its design is associated with a main problem which is the string stretch because continuous wire ropes have relatively lower elastic modulus comparing to CSRs as it can be seen in table 6.

The phenomenon of stretching causes a decrease in the effective stroke of the plunger because of the lag between the polished rod and the plunger movements. This is better described through the Displacement vs Time graph of the plunger (blue) and the polished rod (green) in figure 25 below.

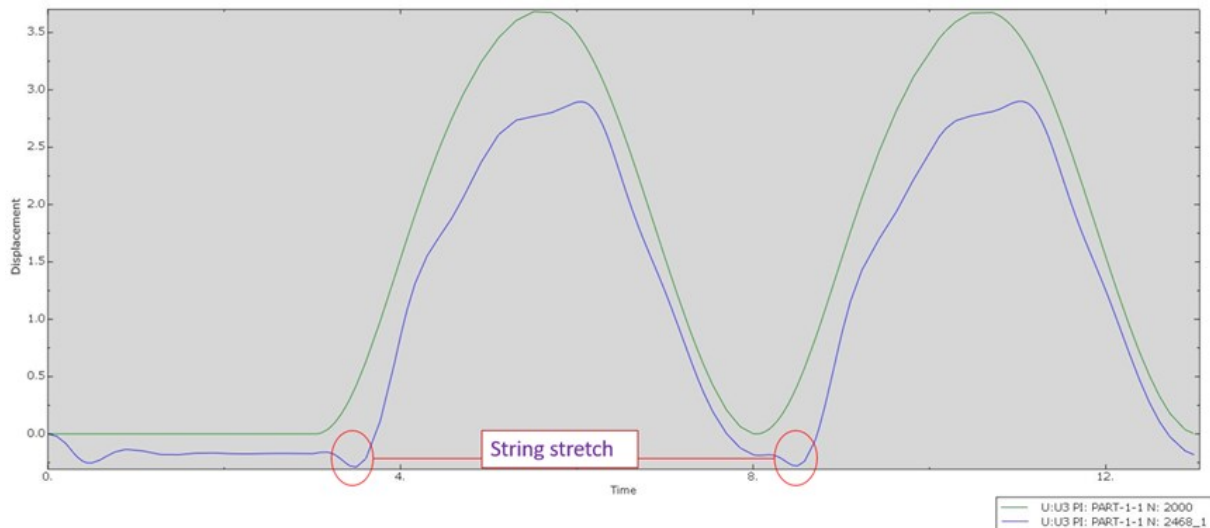


Figure 25: String Stretch of continuous ropes [20]

In this case, a wire rope was used for the simulation and the analysis of the graph indicates the following:

The wire rope is slightly stretched due to its self-weight before the start of the upstroke. Afterwards, as the upstroke starts, the rope is stretched more and the plunger stroke starts after about 1 second delay compared to the polished rod. This causes a delay in the down stroke as well. The phenomenon of string stretching is even more problematic when implemented in vertical wells or in the case of using bigger plungers.

In order to resolve such problems, conventional pumping units must be replaced by newer pumping systems. Hydraulic Units are thought to be a perfect substitute as it allows for relatively longer strokes. This increase in surface stroke will definitely improve the effective plunger stroke and maximize production rates. Furthermore, this unit is adaptable to operate at different pumping speeds during up and down stroke phases, which means fewer rope stretch cycles and better wear distribution. This leads to maximization of the runtime of the downhole equipment. [21]

In order to analyze the performance of the hydraulic unit, the simulation model considers both CSR and wire rope string. Both case studies are described in the following two chapters respectively.

5.6 Case Study 3: Hydraulic Pumping Unit / CSR String

In case study 3, the performance of the proposed pumping unit was tested and analyzed when running with conventional rod string at the same wellbore conditions and pumping regime already described in case study 1. Fulfilling these conditions, the simulation results can be then used to highlight the advantages and improvements added to the pumping operations when traditional rod pumping systems are replaced by such a new long stroke hydraulic pump.

In this chapter, the simulation process using Simulink/Matlab software is explained in details. The Simulation process includes: model building, blocks configuration, valve commands implementation and polished rod load insertion.

5.6.1 Model Building

Construction of the proposed model using Simulink/Matlab Software is the first step of the simulation process. It consists of linking all functional components of the hydraulic system together following a predefined architecture. All necessary components such as pumps, hydraulic cylinders and valves can be found in the software library as shown in figure 26.

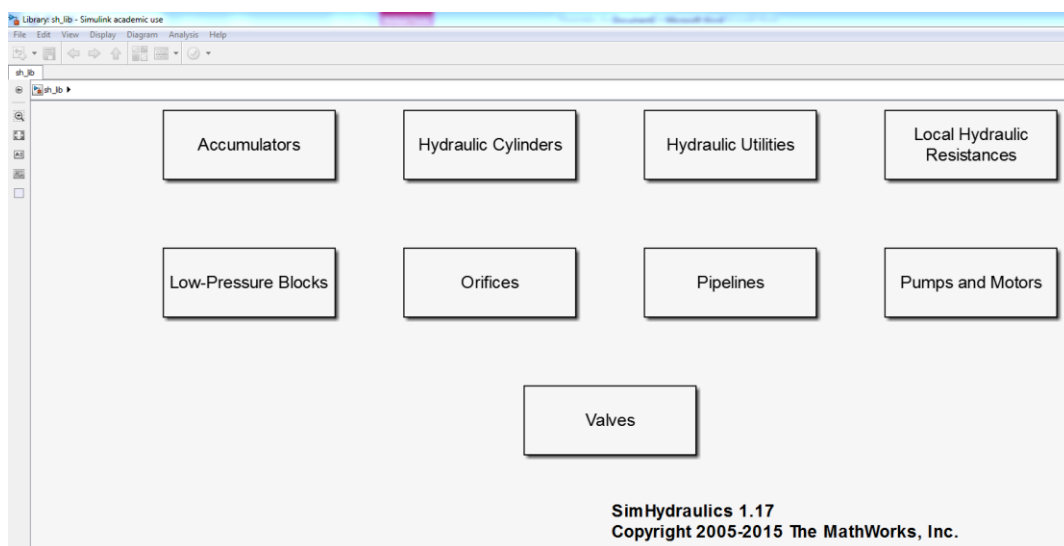


Figure 26: Simulink Blocks Library

The key components of the proposed hydraulic unit are:

- Double acting hydraulic cylinder
- 4-way directional valve
- Variable displacement pump

These blocks are linked together along with other components to form the hydraulic circuit of the pumping unit as shown in figure 28.

The operation of each of the presented components as well as the working principle of the overall pumping system can be briefly described as follows:

The primary energy is delivered to the system through an angular velocity source that generates velocity differential at its terminals. The generated power is extracted by the variable

displacement pump and delivered to the hydraulic fluid. The pump displacement varies depending on the physical control signal (block C) to which it is connected. Now the hydraulic fluid is directed at the desired pressure and flow rate to the 4-way directional valve. This control valve has four ports and three flow paths. The ports P, T, A and B are connected respectively to the hydraulic pump, storage tank and the two sides of the double acting hydraulic cylinder. Depending on the input signal of valve commands applied through the ports SA and SB, the fluid can flow from the pump to the actuator via flow paths P-A or P-B and back from the hydraulic cylinder to the storage tank via paths A-T or B-T. The configuration of the valve signal commands and their influence on the operational behavior of the directional valve is further discussed in section 5.6.3.

At this stage, the hydraulic fluid is directed to the double-acting hydraulic cylinder where the hydraulic energy is converted to mechanical energy in the form of translational motion. The reciprocating motion of the piston inside the hydraulic chamber will be in turn transferred to the polished rod via a set of pulleys and finally a vertical reciprocating pumping action is obtained. The hydraulic cylinder is equipped with snubbers (cushions) on both its ends in order to allow for hydraulic braking in case of sudden increase in the piston velocity due to well load changes. The cushioning tends to absorb some of the kinetic energy of the hydraulic fluid and prevent the occurrence of velocity peaks within the system [26]. The cushioning device is presented in figure 27 below.

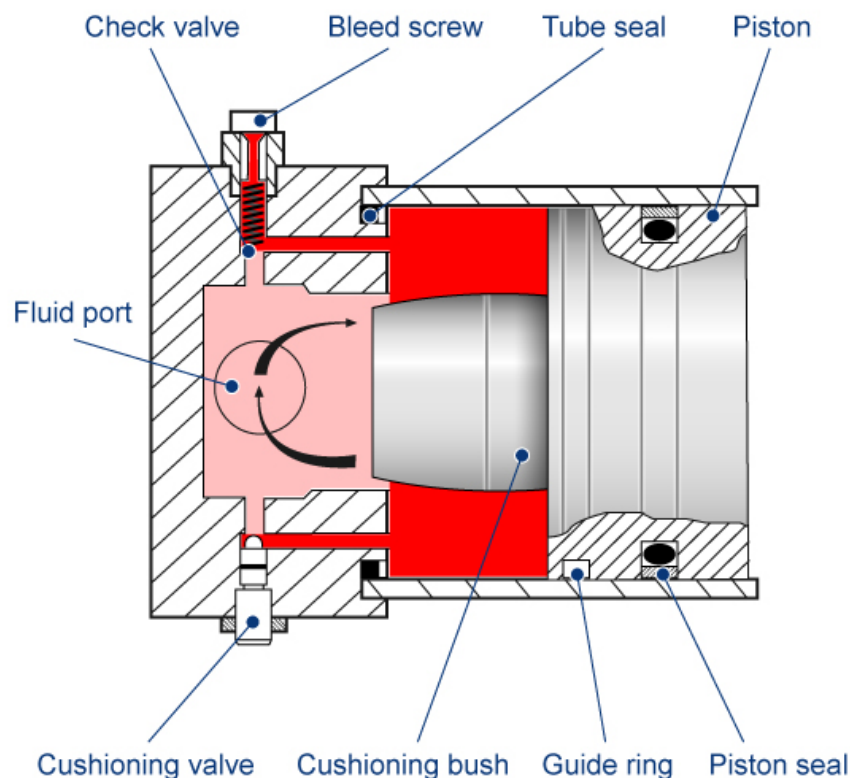


Figure 27: Schematic of the Cushioning Device [26]

At the end of the stroke, the cushioning bush blocks the flow of the hydraulic fluid, which becomes restricted to flow only through the cushioning valve (lower orifice). The flow restriction results in a pressure increase in the cylinder, which help decelerating the movement of the piston instead of hard tapping on the cylinder wall. When the flow is reversed to begin the second stroke, the fluid enters through the fluid port and is directed initially through the check

5.6.2 Blocks Configuration

So far, the main model structure is built. Now, it is necessary to configure each of the circuit components in order to ensure efficient and smooth pumping operation.

The basic simulation parameters are summarized in table 7 below:

Table 7: Configuration of main Unit Components – Case Study 3

| Component | Parameter | Value |
|--------------------------------|---|-------|
| Hydraulic Pump | Max displacement (l/rev) | 2 |
| | RPM | 1200 |
| | Nominal pressure (MPa) | 7.2 |
| 4-way Directional Valve | Maximum orifice area (cm ²) | 10 |
| | Discharge coefficient | 0.7 |
| Hydraulic Cylinder | Piston stroke (m) | 8 |
| | Piston area A (cm ²) | 24 |
| | Piston area B (cm ²) | 19 |

Table 12 in appendix E shows the parameter configurations of all hydraulic system components for both case studies 3 and 4.

5.6.3 4-Valve Signal Commands

Valve commands¹ in figure 28 is the control signal of the 4-way directional valve. As already described in the literature, the directional valve receives the flow from the hydraulic pump through port “P” and directs it to the hydraulic cylinder through ports “A” and “B” in an alternating way in order to achieve the reciprocating strokes of the piston. This means that the stroke length and the pumping speed (strokes/min) can be controlled by adjusting the frequency of the control signal of the directional valve (which is the trapezoidal signal in this case). In other words, in cases where increased stroke length is recommended for better pumping performance, this adjustment is easily done by decreasing the signal frequency: this will allow the directional valve to inject hydraulic fluid from the same port (same chamber) for a longer time leading to an increase in the piston displacement. The opposite case is also possible when shorter strokes are required, then the solution is increasing the signal frequency.

The design of the control signal for the case study 3 is presented in figure 29 below:

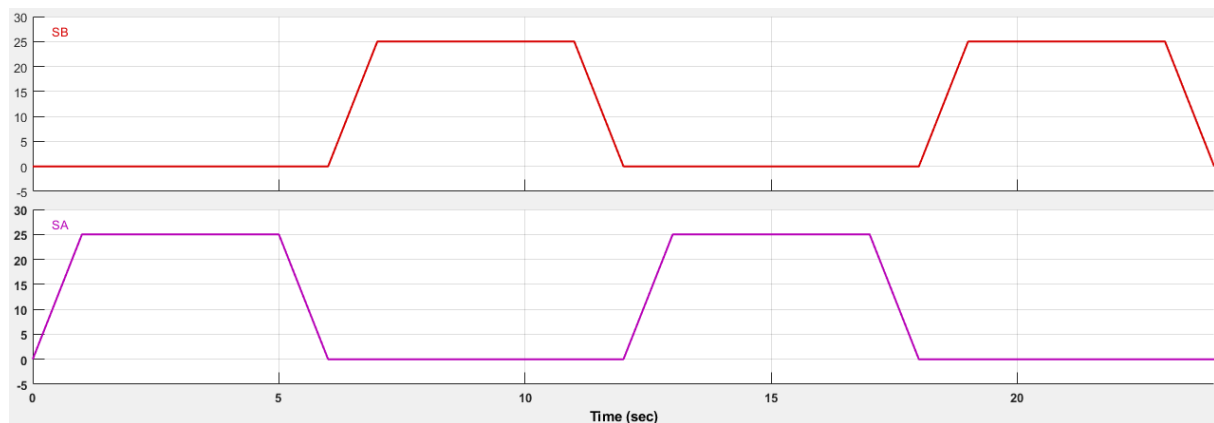


Figure 29: Valve Control Signal - Case Study 3

The valve control signal shown in figure 29 represents the equivalent speed curve signal that is applied to the hydraulic pumping unit along two pumping cycles. In other words, in order to get comparable results with the conventional sucker rod pump that is described in case study 1, the current hydraulic unit is designed to run under the same pumping regime. Therefore, it can be seen from the control signal graph that one full stroke lasts 12 seconds which means that the pumping speed of the hydraulic unit in this case study is 5 SPM.

It is important to mention that target polished rod velocity is proportional to the rate of the fluid that is delivered to the hydraulic actuator. At the beginning of the stroke, the velocity is zero and a certain maximum velocity needs to be reached (1.2 m/sec for instance): this interval from zero to 1.2 m/sec represents the acceleration phase in which the velocity is increasing gradually. In order to obtain this velocity increase, the fluid rate should be increased gradually as well until reaching the target velocity. The fluid rate is controlled through the configuration of the valve control signals.

The signal configuration for the full pumping cycle is finally obtained and it contains an accelerating phase, a constant speed phase and finally a decelerating phase for the upstroke, which is represented by the purple curve in the graph (SA), and the same is repeated for the down stroke, which is illustrated in the red curve (SB).

5.6.4 Polished Rod Load Implementation

In order to simulate the dynamic forces that the polished rod and the rod string experience in the wellbore, the polished rod loads are applied to the hydraulic cylinder of this pumping unit using the “force source” and “Signal1” blocks that can be seen in figure 30.

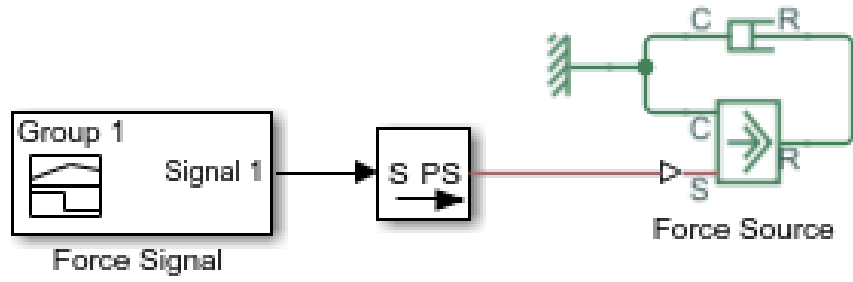


Figure 30: Block Diagram for Polished Rod Load Simulation

Following the same procedure as in case study 1 and case study 2, the simulation results from Abaqus corresponding to the polished rod load of the conventional unit running with conventional rod string were converted to load versus time dataset and then implemented into the hydraulic pump model through the force signal block shown in figure 30.

Figure 31 below illustrates the polished rod load behavior over 24 seconds, corresponding to two full strokes.

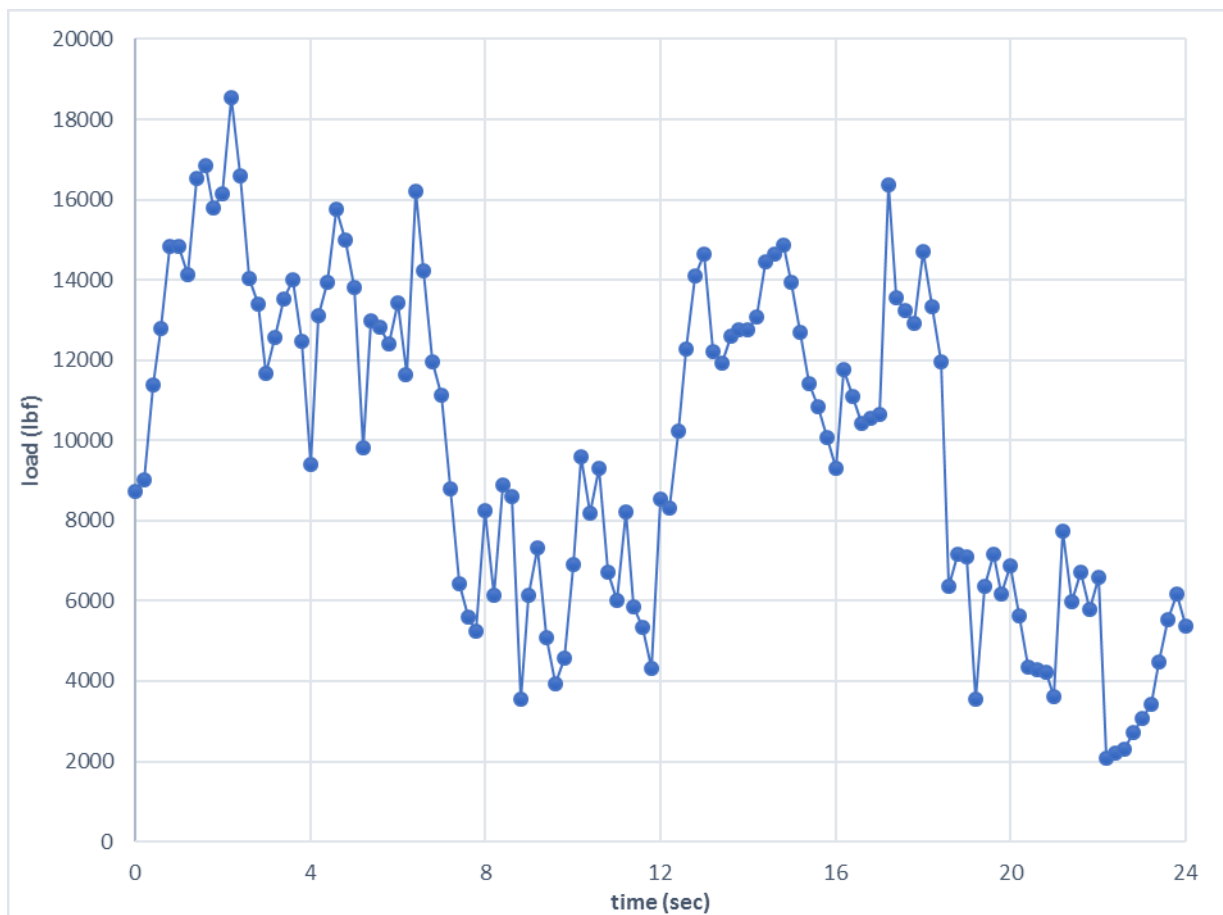


Figure 31: Polished Rod Load Curve – Hydraulic Unit with CSR String

5.7 Case Study 4: Hydraulic Pumping Unit / Continuous wire rope

In this case study, the proposed hydraulic unit is running using continuous wire rope string instead of conventional sucker rod string, however the overall hydraulic circuit structure is kept the same as in case study 3 (figure 28).

5.7.1 Blocks Configuration

In this case, study the parameter configuration of the main hydraulic system components is kept the same as it can be seen in table 8. However, other parameters were slightly modified such as the control signal of the angular velocity source and the fixed orifice size. The full comparison between the parameter configurations of both case studies can be seen in Appendix E, table 12.

Table 8: Configuration of main Unit Components – Case 4

| Block | Parameter | value |
|-------------------------|---|-------|
| Hydraulic Pump | Max displacement (l/rev) | 2 |
| | RPM | 1200 |
| | Nominal pressure (MPa) | 7.2 |
| 4-way Directional Valve | Maximum orifice area (cm ²) | 10 |
| | Discharge coefficient | 0.7 |
| Hydraulic Cylinder | Piston stroke (m) | 8 |
| | Piston area A (cm ²) | 24 |
| | Piston area B (cm ²) | 19 |

5.7.2 Signal Commands:

The design of the control signal for the case study 4 is presented in figure 32 below:

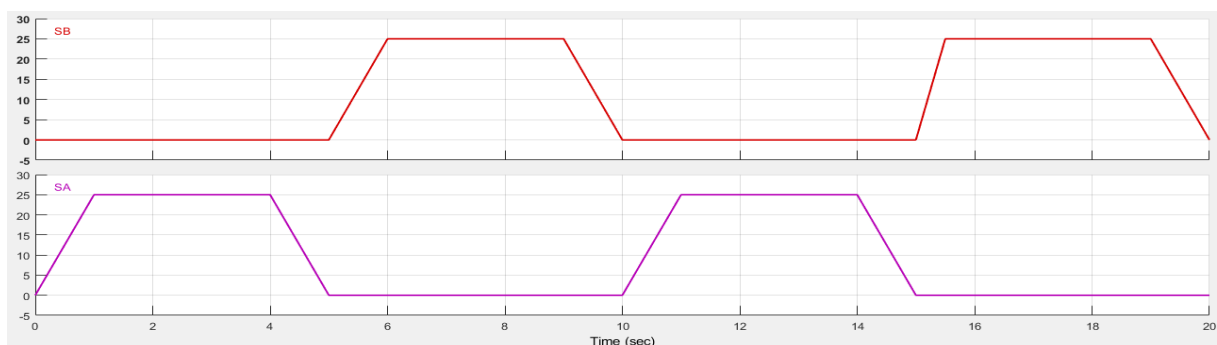


Figure 32: Valve Control Signal - Case Study 4

In this case study, the hydraulic unit operates under the same pumping regime as for case study 2. This can be seen in the control signal graph, the pumping stroke period is 10 seconds therefore, the pumping speed is 6 SPM. The increase in the pumping speed will result in equalization of the productivity between the two case studies 3 and 4 because the latter one uses a SRABS pump with the wire rope having smaller barrel volume comparing to the downhole pump configuration in case study 3.

5.7.3 Polished Rod Load Simulation

In order to test the performance of the proposed pumping unit when it is running with continuous wire ropes, the corresponding simulation results were obtained from Abaqus simulation and converted into load versus time dataset following the same steps discussed before.

Figure 33 below illustrates the polished rod load behavior over 20 seconds, corresponding to two full strokes.

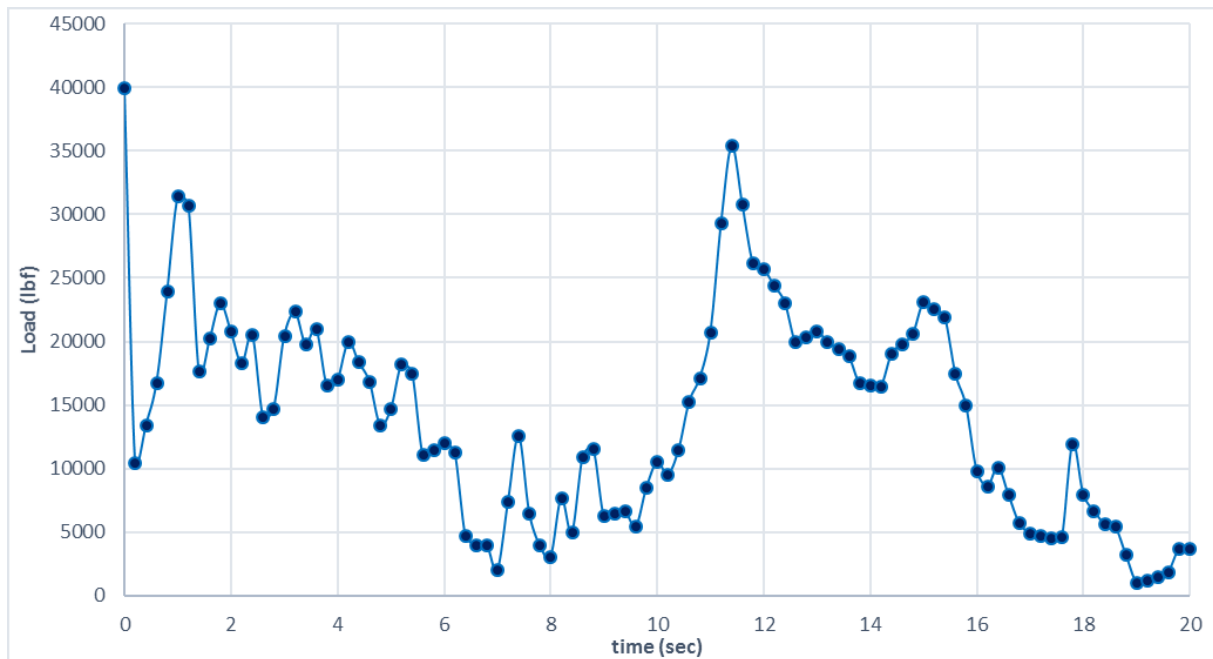


Figure 33: Polished Rod Load Curve - HPU with Wire Rope

6 Simulation Results

Having described the simulation methodology of the proposed pumping unit in the previous chapter, the simulation results will be then presented and analyzed in the following sections. The evaluation of the pump jack performance was done through three main parameters: Pumping unit kinematics, hydraulic pump performance and power consumption.

6.1 Pumping Unit Kinematics

Kinematic behavior is one of the most important criteria in evaluating the performance of any surface pumping unit. Thus, the visual representations of the displacement vs. time as well as the velocity profile of the polished rod are presented and analyzed in the following section.

The simulation results prove that the hydraulic unit could successfully achieve a reciprocating pumping movement with relatively longer strokes than conventional rod pumps. Yet, the effective stroke is still less than the desired one, which is initially set as 8 m. The decrease in the effective stroke is more in the case of wire rope due to the string stretch.

In both case studies 3 and 4, the hydraulic unit proves a good adaptability to operate using different rod strings (CSR string & wire ropes).

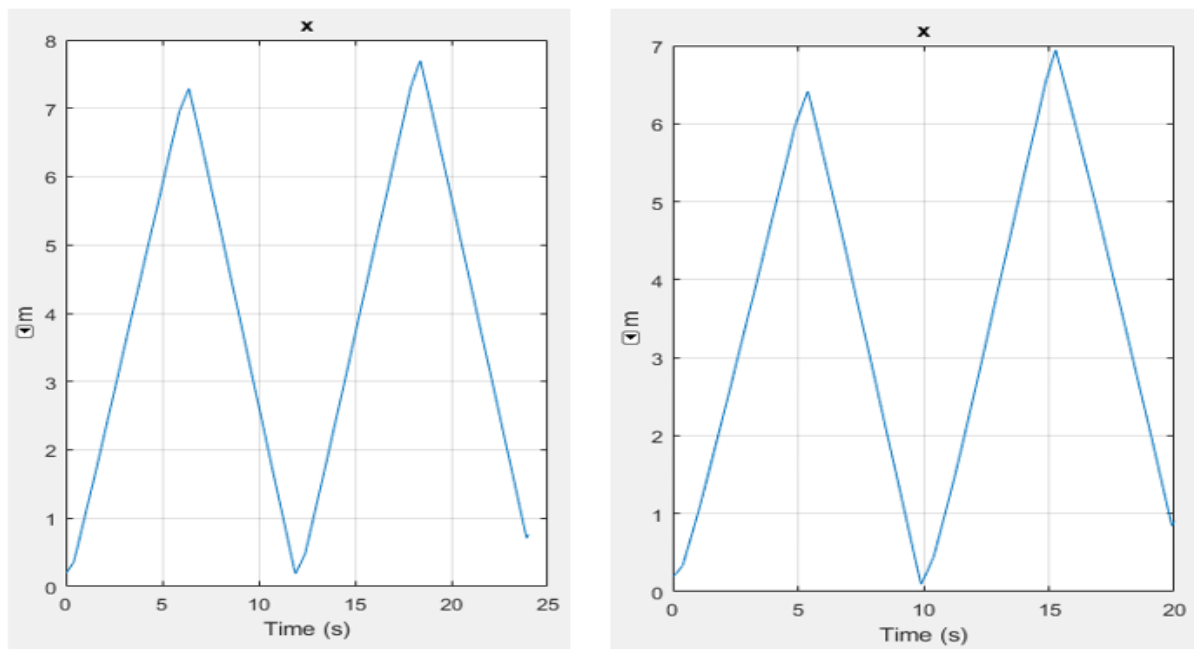


Figure 34: Polished Rod Load Displacement (Left: Case 3 – Right: Case 4)

According to the polished rod displacement curve in figure 34, the simulated pumping unit proves its capability to achieve relatively longer effective strokes. The stroke intervals of the hydraulic actuator are nearly identical to the strokes intervals of the input control signal of the directional valve. In effect, the hydraulic piston achieved one full pumping cycle (upstroke and down stroke) in 12 seconds in the case of CSR String and 10 seconds in the case of wire rope

meaning that the target pumping speeds (6 and 5 SPM respectively) were successfully reached.

One of the most important parameters that the graph indicates is the stroke length. In effect, it can be seen that the pumping unit could provide relatively longer surface strokes between 6.5m and 7.5 m. This will dramatically decrease the effect of wire rope stretching faced when operating with conventional pump jacks that have a stroke length up to 3.65 m. This increase in the surface stroke will also result in an important enhancement in the well productivity

It is important to mention that the modeled hydraulic pump is flexible in terms of pumping speed and not limited to a single pumping regime, which is the case for this simulation. In cases of low inflow performance of the reservoir or stripper wells, slower pumping speed is required in order to avoid over-pumping. Therefore, the unit can be easily reconfigured by controlling the input stroke intervals of the directional valve signal.

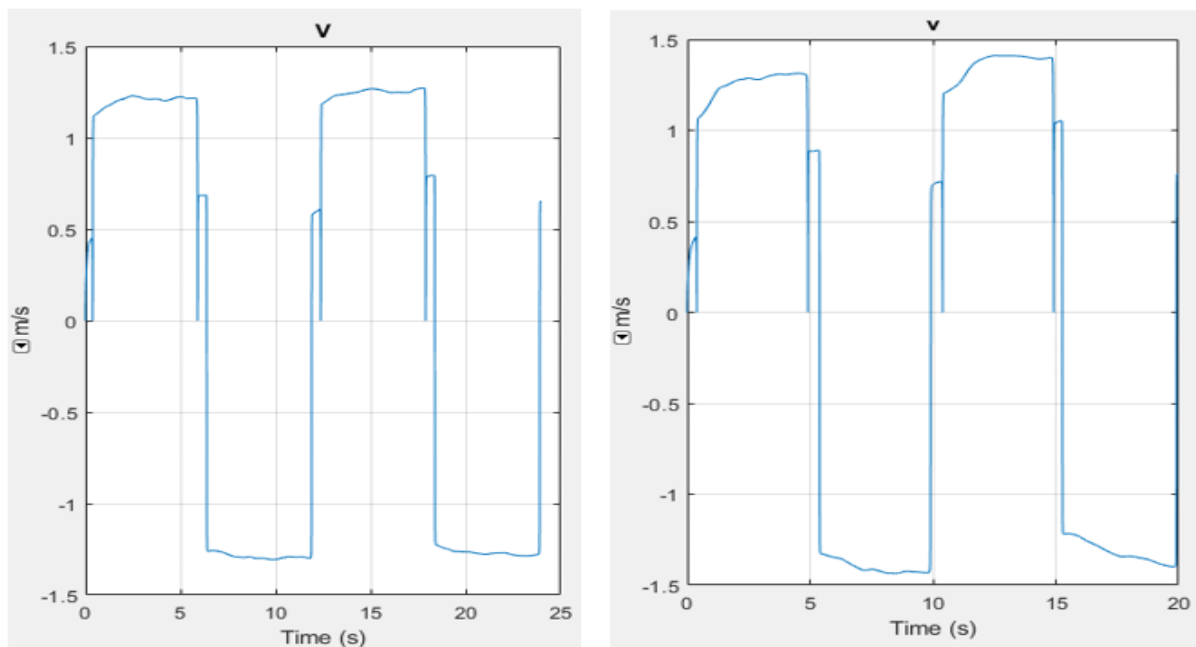


Figure 35: Velocity Profile (Left: Case 3 – Right: Case 4)

The velocity profile of the simulated pumping unit (figure 35) indicates that the speed of the hydraulic piston is slightly higher during the upstroke phase (approximately 1.2 m/sec) compared to the down stroke phase (1.3 m/sec) in the case of CSR string. This can be explained by the higher well loads experienced by the hydraulic cylinder during the upstroke phase. Hence, the hydraulic energy of the hydraulic pump is mostly converted to potential energy (pressure) that is used to overcome these loads. This is inverted during the down stroke phase as the well loads decrease, therefore, the required pressure decreases and the hydraulic piston travels at higher velocity.

In the case of wire rope (case study 4), the pumping unit is running - as designed in section 5.7.2 – at higher speed compared to case study 3. Yet, the pumping regime of 6 SPM is still

considered a relatively slow regime which is beneficial to the wire rope in terms of reducing stretch cycles and avoiding high inertia that cause load fluctuations and shocks.

The shock loading at the end of the strokes is a common problem that is associated with hydraulic cylinders and consists of sudden impact of pressure waves due to abnormal loads that might arise within the system. The loads are not only caused by the high fluid pressure but also due to the kinetic energy of the moving parts of the cylinder (e.g. hydraulic piston). hence, reducing the pumping velocity of the unit will drastically eliminate these end stroke shocks.

Moreover, running at low pumping speed regime especially during the down stroke phase will dramatically decrease the compressive forces acting on the sucker rod string and therefore eliminating the risk of buckling. Therefore, operating at this regime or even at slower speeds leads to an increase in the MTBF.

During the shift from the upstroke to down stroke and vice versa, the hydraulic cylinder experiences sudden high-pressure shocks resulting in a dramatic increase in the piston velocity. In order to overcome these shock effects, the hydraulic cylinder is incorporated with snubbers in both ends as mentioned already. The effect of these snubbers can be seen in the velocity profiles of pumping unit: In effect, the snubber forms a cushion that absorbs the load shocks resulting in cancelling of the velocity peaks that might occur at the extremities of each stroke. Instead of velocity peaks, the velocity profiles show short intervals with lower velocities.

6.2 Hydraulic Pump Performance

Examining the hydraulic pump performance is incredibly important when judging the overall system efficiency for two main reasons: firstly, the hydraulic pump is the primary energy source as it provides the hydraulic chamber with the required fluid rate and pressure to achieve its stroke. Secondly, calculating the pressure and rate of the hydraulic pump will allow determining the energy requirements of the pumping unit.

As expected, the variable displacement pump shows a great response to the input signal variations. In effect, the pump flow rate is proportional to the signal of the directional control valve. This pump behavior has a great contribution in overcoming the problem of energy efficiency associated to hydraulic systems since the pump is controlled to produce energy whenever needed. As a result, no energy is wasted when no work is required.

Figures 36 and 37 show the hydraulic pump flow rate and pressure behaviors for both case studies 3 and 4.

By examining both curves together, it can be concluded that during the upstroke, the pump delivers less flow rate at high pressure and the opposite occurs during the down stroke. This proves what has been already explained during the discussion of the velocity profile.

The cushioning effect can be also seen in these figures where the flow rate is minimized at the end of every stroke as the cushion bush (figure 27) blocks the main orifice and fluid is restricted

to flow through the cushioning valve. As a result, the fluid is pressurized between the piston and the cylinder wall at the stroke extremity leading to pressure peaks that appear figure 37.

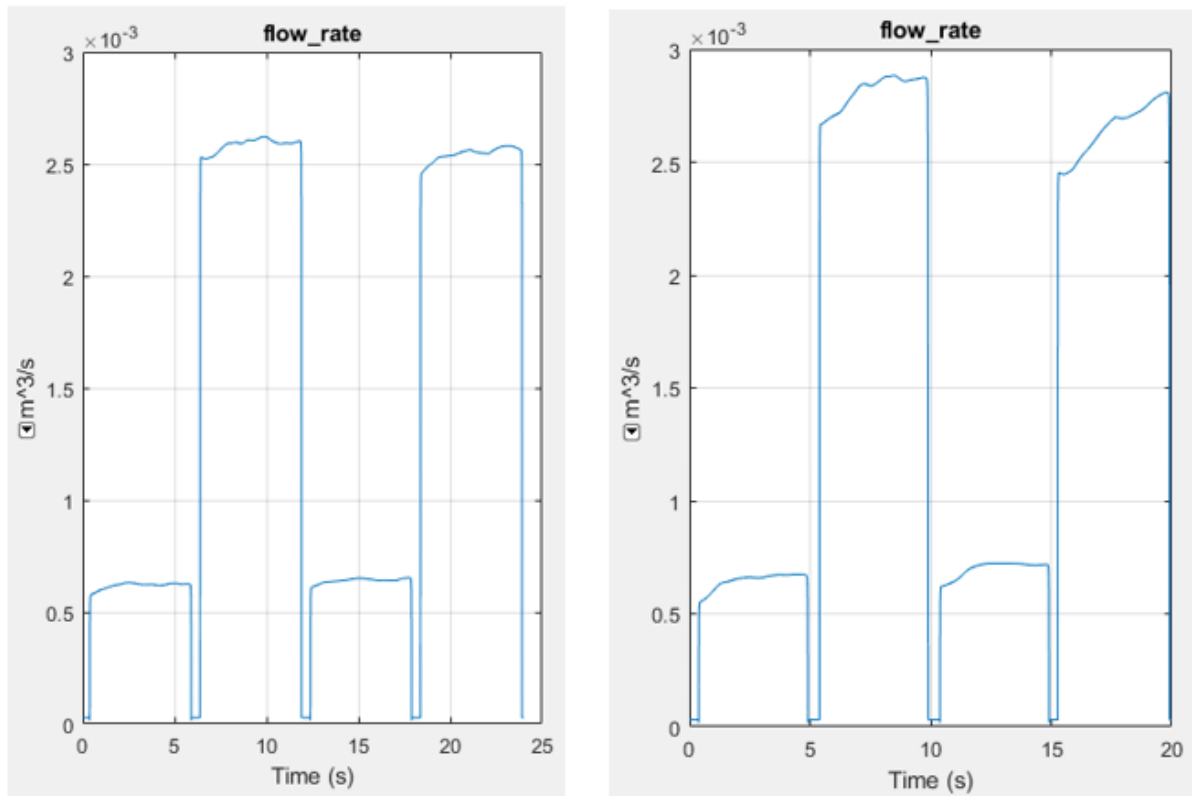


Figure 36: Hydraulic Pump Flow Rate - Case Studies 3 & 4

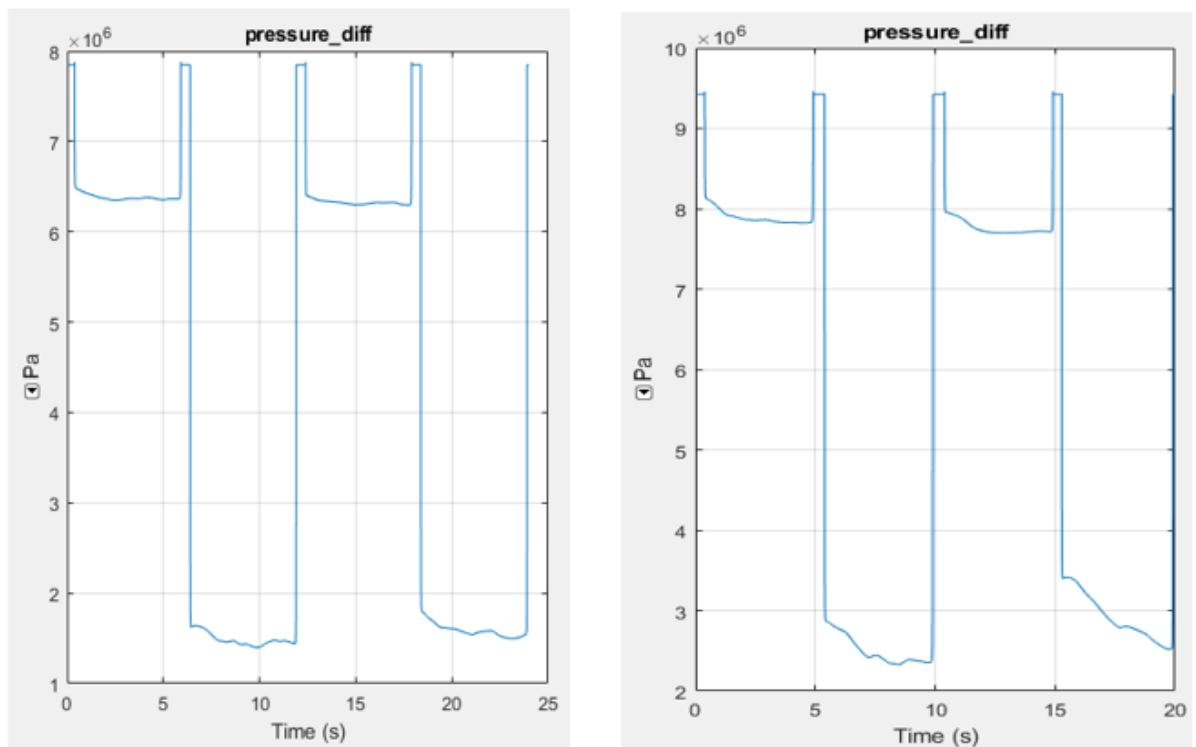


Figure 37: Hydraulic Pump Pressure – Case Studies 3 & 4

6.3 Hydraulic Pump Power Consumption

In this chapter, the energy efficiency of the proposed hydraulic pumping unit is studied for both case studies 3 and 4 through the power consumption curves of each of them and with comparison to power consumption of their corresponding case studies 1 and 2 respectively.

Figure 38 below represents the mechanical power consumption of the each of the pumping systems over two pumping cycles.

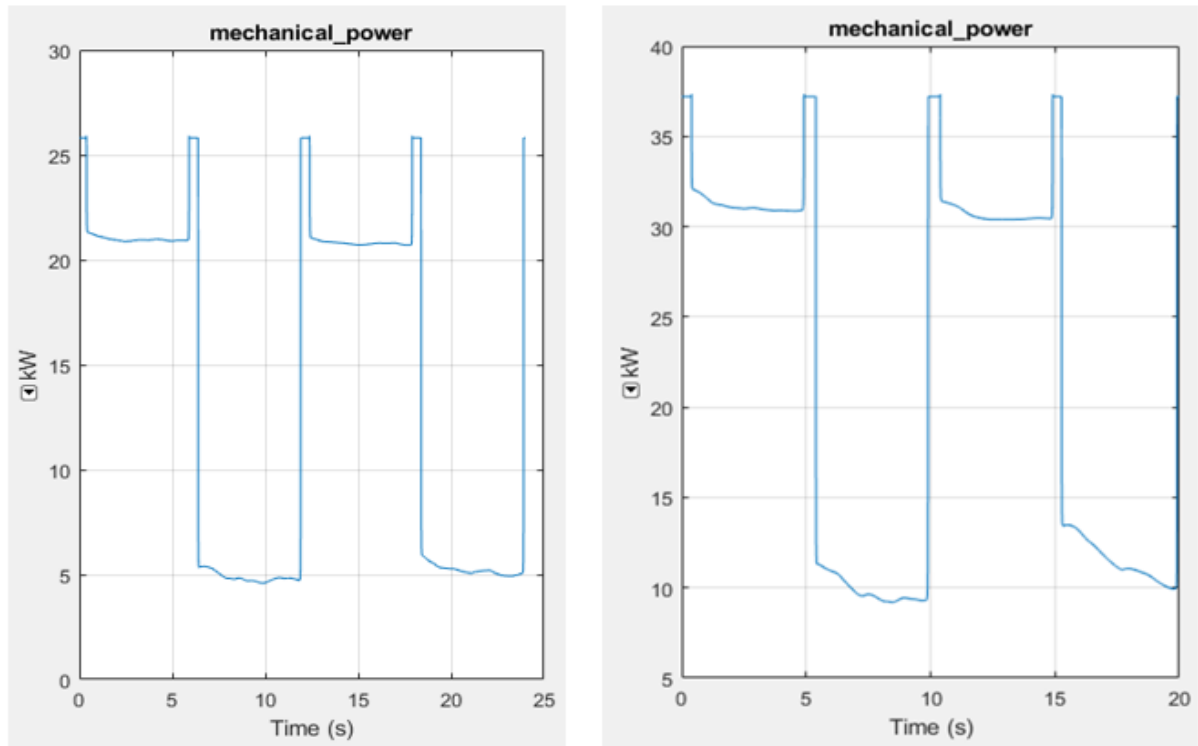


Figure 38: Power Consumption of the Hydraulic Unit (Left: CSR string /Right: Wire Rope)

The simulation results of both case studies 3 and 4 in figure 38 can be analyzed as follows:

The power consumption magnitudes of the pumping unit during the upstroke and down stroke can be averaged to 19.73 kW for case study 3 and 30.91 kW for case study 4.

The power consumption is maximum during the acceleration of the upstroke phase, afterwards it decreases during the uniform phase and finally reaches its minimum at the down stroke phase.

Despite implementing a cushioning device that tends to cancel the shock loads at the stroke-ends, short intervals of peak power consumption still appear at the extremities of the strokes. This is because the working principle of the cushioning device consists of converting the kinetic energy of the piston into potential energy (in form of pressure). Hence the energy still exists but just in other form and the power unit must deliver it anyway.

The power consumption behavior of the pump highlights the advantage of using a variable displacement pump instead of standard pumps, as the energy delivered to the system is always approximately equivalent to the system requirements. In effect, it can be seen in figure 37 that the difference between the upstroke and down stroke is quite large, meaning that no extra energy is used when not needed.

6.4 Performance Comparison with Conventional Units

In this chapter, the simulation results of the proposed pumping unit and CSR are summarized and compared for each case study.

The polished rod displacement corresponding to the four case studies are visualized in figures 39 and 40 below.

The major advantage that can be concluded from this graph is the capability of the proposed hydraulic pumping unit to provide longer surface strokes than conventional pump jacks regardless of the downhole setup of the sucker rod string and downhole pump.

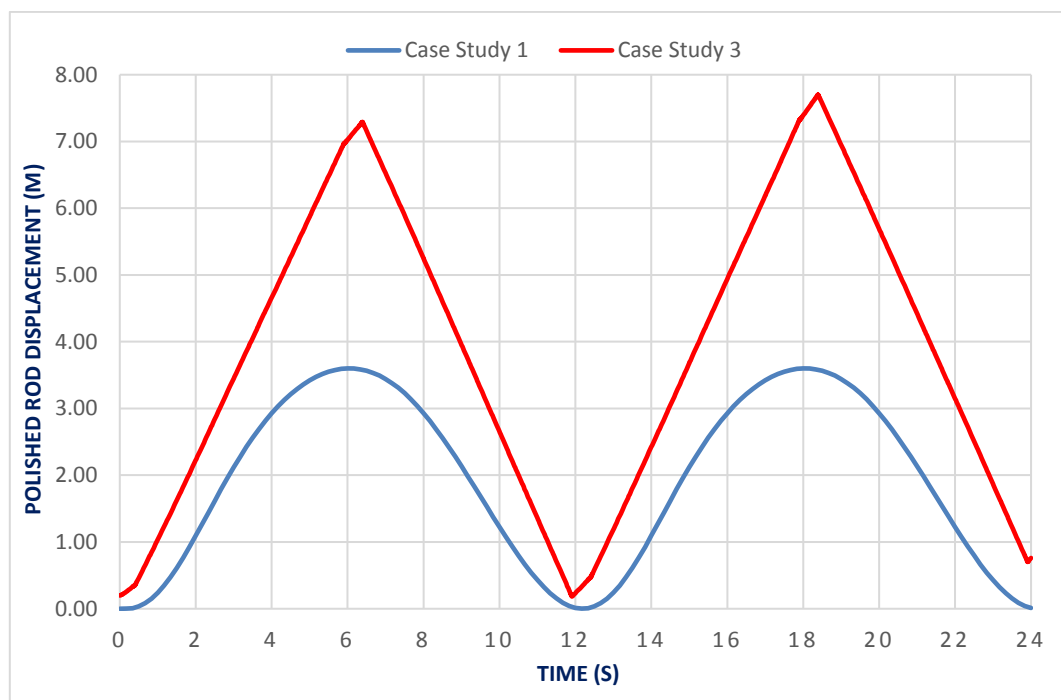


Figure 39: Polished Rod Displacement of Case Study 1 & 3

When running with CSR string (Figure 39), substituting the CSR pump with the proposed hydraulic unit has increased the effective surface stroke of the polished rod from 3.66 m to approximately 7.3 m. However, in the case of wire rope (figure 40), the effective stroke has increased from 3.66 m to approximately 6.6 m.

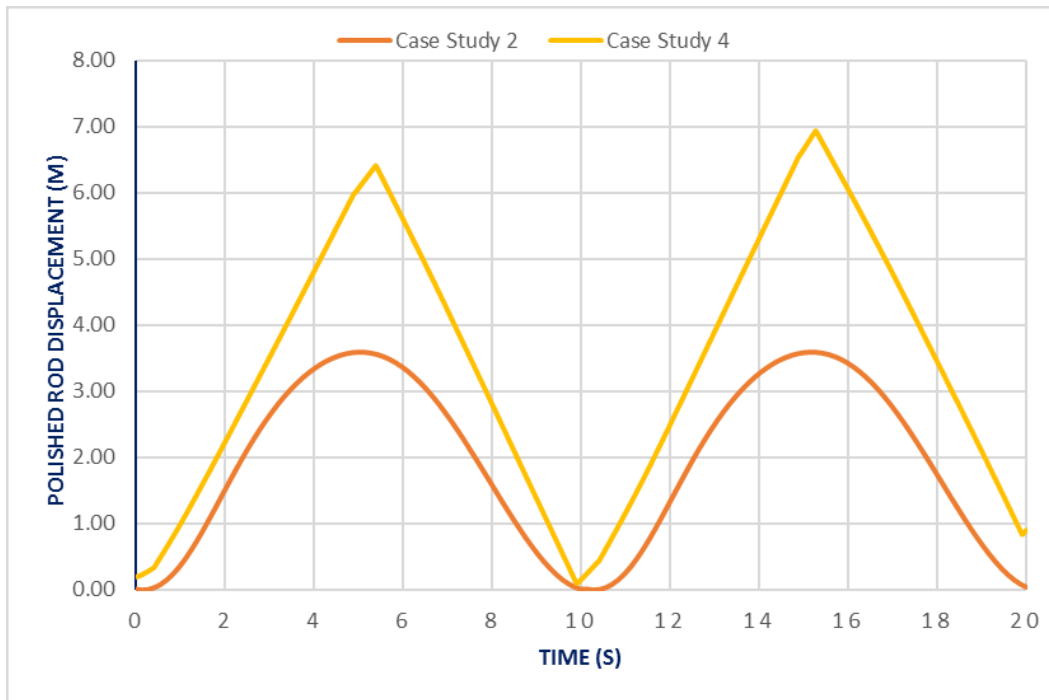


Figure 40: Polished Rod Displacement of Case Study 2 & 4

The comparison between the polished rod velocities of the different pumping units can be seen in figures 41 and 42.

Bearing in mind that the hydraulic pump performs longer strokes than the conventional pump, however, it could successfully achieve the full pumping cycle within the same period as the conventional unit. This is thanks to the fact that using the trapezoidal velocity profile; the polished rod reaches its maximum velocity (m/sec) faster than in the case of sinusoidal velocity profile. The advantage of the trapezoidal velocity curve over sinusoidal curve was discussed in more details in chapter 6.1.

Moreover, it can be seen in the velocity curves of the hydraulic unit that the constant velocity phase is the most dominant over the pumping cycle. This results in dramatic decrease in the inertial forces in the wellbore and helps in reducing the load and pressure fluctuations. However, in the case of CSR unit it is clear that the polished rod velocity is progressively increasing and decreasing without any constant phase periods. This means that the inertial forces are always present and acting on the polished rod and rod string promoting the risk of string stretch and even failure in the worst case.

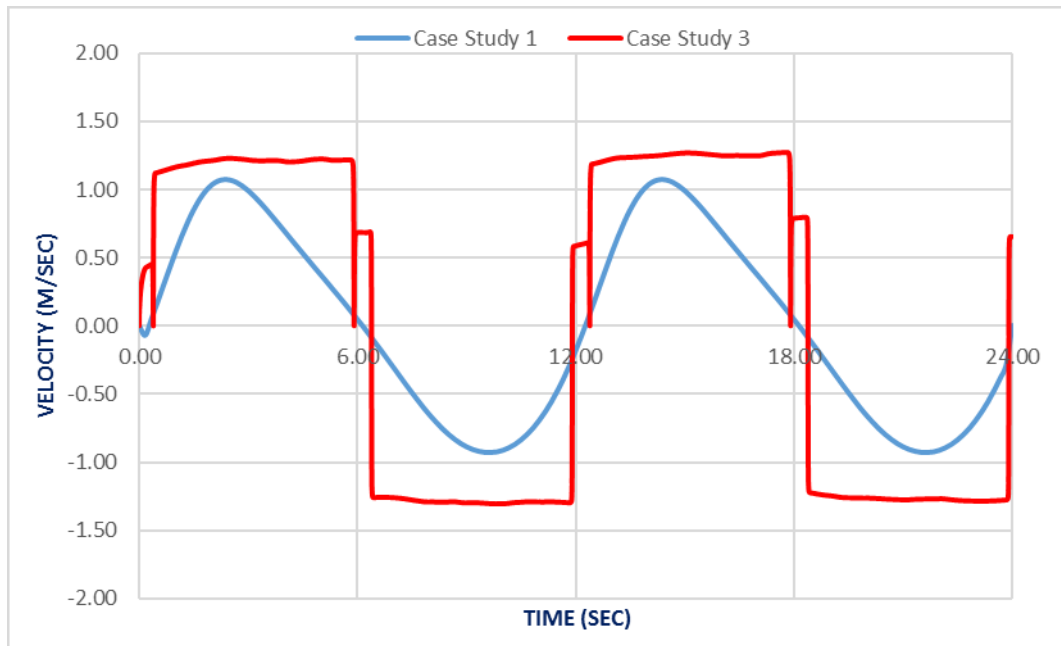


Figure 41: Polished Rod Velocity - Case Study 1 & 3

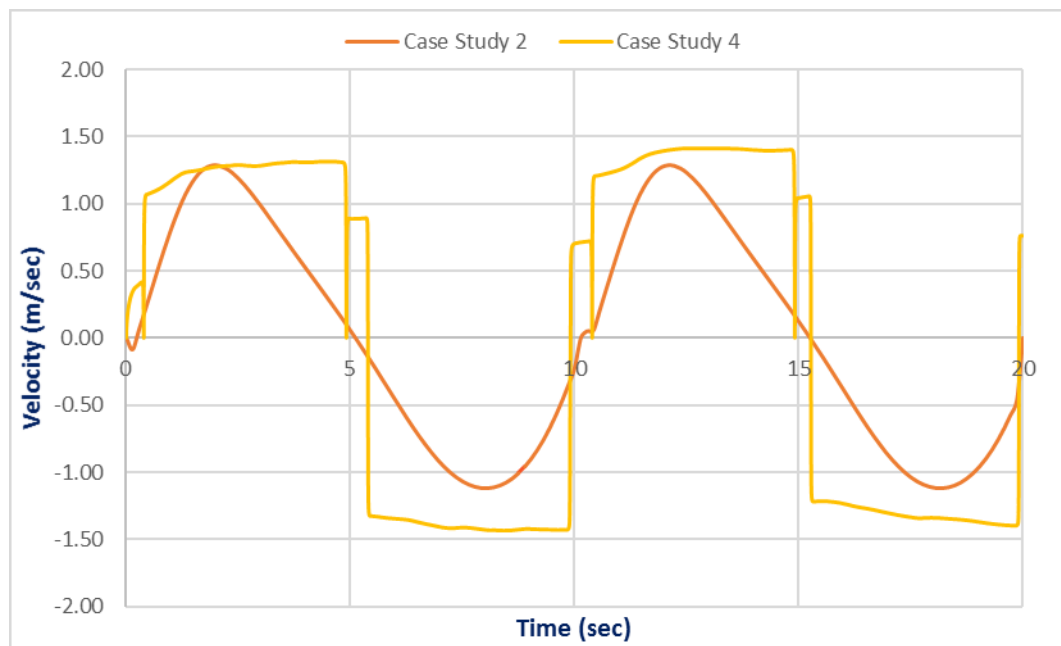


Figure 42: Polished Rod Velocity - Case Study 2 & 4

The comparison between power consumption of the hydraulic unit running with conventional rod string and wire rope is shown in figure 43.

The graph indicates that the power consumption of the proposed pumping unit running with the conventional downhole setup (case study 3) is slightly lower than the case of continuous wire rope and SRABS pump (case study 4). This can be explained by the higher loads experienced in the case of wire rope configuration. In effect, it can be seen in the load profile of case study 4 that the wire rope is suffering from more load fluctuations that are resulting from its elastic behavior as well as the high inertial forces of the wellbore fluids.

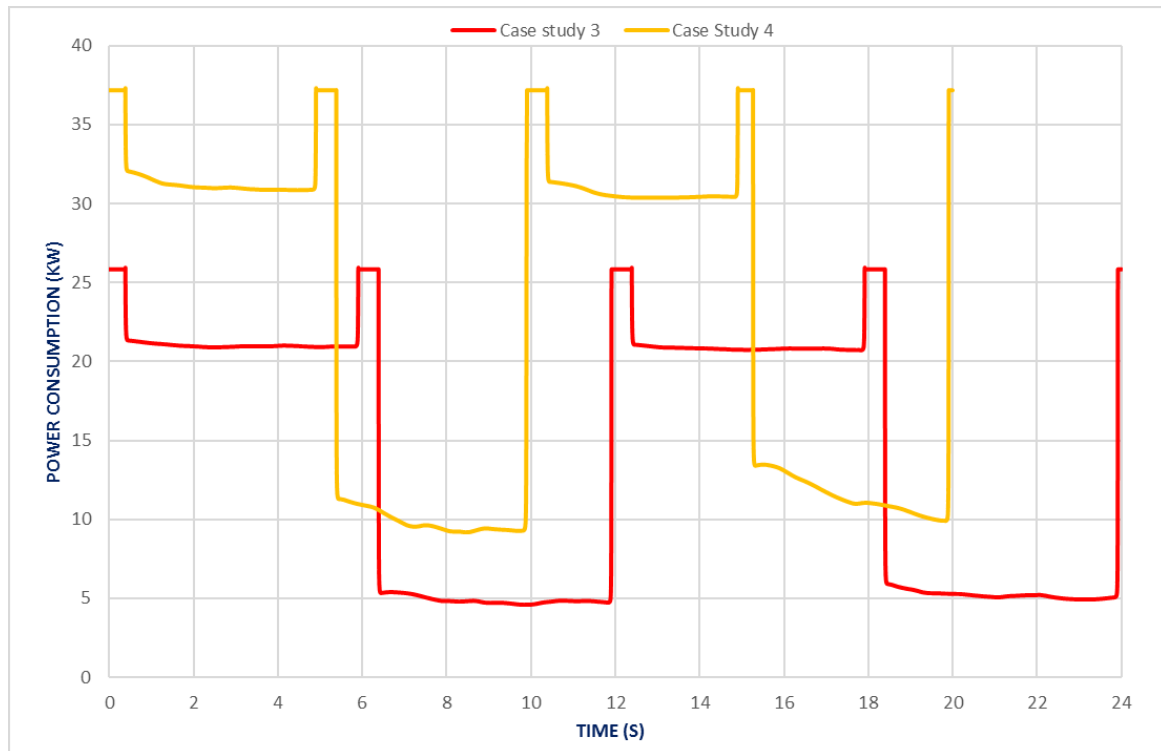


Figure 43: Power Consumption of the Modeled Pumping Unit

The summary of all relevant results obtained from the simulation of the four case studies is attached in table 9 below.

Table 9: Summary of Results of the Four Case Studies

| Parameter | Unit | Case Study 1 | Case Study 2 | Case Study 3 | Case Study 4 |
|----------------|------|--------------|--------------|--------------|--------------|
| Surface Stroke | m | 3.66 | 3.66 | 7.3 | 6.6 |
| Working period | s | 12 | 10 | 12 | 10 |
| Pumping Speed | SPM | 5 | 6 | 5 | 6 |
| Power | kW | 16.53 | 36.07 | 19.73 | 30.91 |

The summary of results presented in table 9 reveals the unique features of the simulated hydraulic unit: In the case of CSR string, it can be seen that the proposed unit delivers twice the surface stroke length of the conventional pump jack, yet the power consumption is slightly increased by only 19%.

The results of the hydraulic unit with the wire rope are even better with an increase by 80% in the surface stroke and a decrease by 15% in the power consumption. This makes the proposed pumping unit an excellent substitute to the CSR pumping unit especially when running with

wire ropes as sucker rod string as it can deliver approximately twice the production rate with less energy requirements.

7 Conclusion

Inspired by several previous hydraulic pumping units, a new design of a long-stroke hydraulic pumping system was modeled and Simulated using Simulink/Matlab Software. The main goal of these innovations is to promote the controllability of sucker rod pumping operations in terms of stroke length and pumping speed (SPM). In addition, the adaptability of the proposed hydraulic unit with wire ropes as a sucker rod string was also tested in the course of this project.

Similarly, to other hydraulic pump jacks, the design of the new pumping system is characterized by significantly smaller footprint and lighter weight compared to conventional sucker rod pumps, making it suitable for sensitive areas such as offshore fields and high-density pads in shale gas reservoirs. Moreover, the minimal infrastructure design and ease of installation make the designed system a perfect candidate as temporary or permanent pumping solution for testing newly drilled wells.

A unique feature of the proposed hydraulic unit is its ability to run with independent up and down stroke pumping velocities that can be easily configured and varied depending on the well inflow performance, wellbore dynamics and target production rates. The configuration flexibility includes the control of stroke lengths as well.

The flexibility of the hydraulic system in terms of stroke length and pumping speed makes it adaptable to operate with wire ropes as a sucker rod string. In effect, the main problem of the wire ropes when implemented with CSR pumping unit is the string stretch, which reduces the downhole pumping efficiency and accelerates the failures of the string. These limitations can be mitigated using the long stroke hydraulic unit running at low SPM regime resulting in no significant stretch cycles relative to the stroke length and improved downhole plunger stroke.

Implementing wire rope as a SR string with the proposed hydraulic unit is very advantageous thanks to its lighter weight; resulting in less counterweight requirements, hence less energy consumption. However, operating with such a string is quite delicate due to its high response to loads variations and fluid inertia in the wellbore. Therefore, an appropriate pumping regime control is decisive in ensuring a secure and efficient pumping operation.

The simulation results indicate that for case study 4, the power consumption of the proposed pumping unit was reduced. Yet, the stroke length was much higher comparing to conventional pumping units. For case study 3, a slight increase in the power consumption was recorded, on the other hand the stroke length was doubled.

The simulation results of the designed hydraulic unit need to be proved by on-site measurements of the operational parameters at wellbore conditions. In addition, some uncertainties associated to the wire rope simulation using Abaqus software need to be overcome by more proper modeling in order to obtain better load dataset that are reliable for this unit.

8 Recommendations

The proposed pumping unit design could successfully meet the objectives initially set such as long pumping strokes, precise control of the strokes intervals and energy conservation. However, there are still some limitations and concerns that were encountered during the simulation and analysis of the hydraulic system. Further improvements and more sophisticated investigations should be performed in the future in order to avoid these deficiencies and optimize the pumping operation using the proposed pumping system.

8.1 Wire Rope Simulation Improvements

For the time being, the knowledge on the wire rope characteristics is still limited to due to the lack of experimental data. Therefore, it is recommended to perform more laboratory tests on these materials under wellbore conditions in order to increase the precision of input data such as friction factors, elastic behavior of the wire rope and effect of fluid flow on the continuous string.

8.2 Design Improvements

One of the main problems that was faced during the simulation process is the sharp increase in the polished rod velocity and power consumption during the shift from the acceleration phase to the uniform phase (constant speed). In order to avoid such problems, the trapezoidal velocity curve should be slightly modified toward smoothing the transitions where the acceleration phases begin or ends. The modified curve, also called S-curve move profile [23], combines the advantages of both trapezoidal and sinusoidal profiles.

The suggested S-curve velocity profile can be seen in figure 44 below.

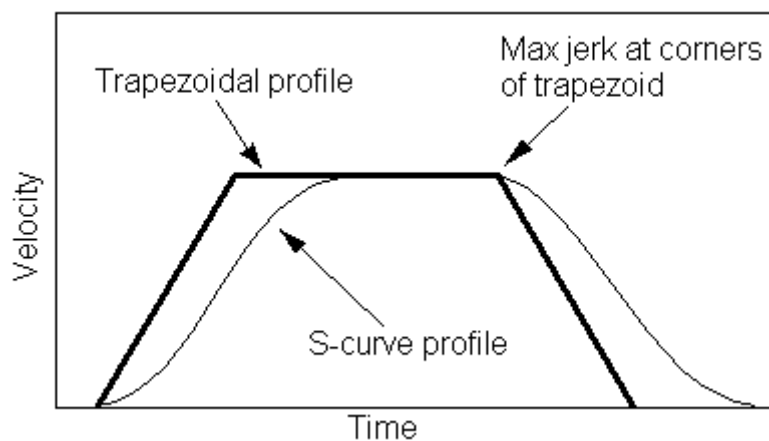


Figure 44: S-curve Velocity Profile [23]

Implementing such a modification to the design of the input signal of the directional valve will help to avoid the jerks that might occur in the polished rod velocity curves, hence smoother pumping movement and more importantly the dramatic decrease in the resultant power consumption.

8.3 HSSE Aspects

Operating with hydraulic systems is generally associated with some typical problems such as the generation of high-level noise and the high risk of oil leaks especially when dealing with high-pressure components such as a hydraulic cylinder. These two problems are critical from the HSSE point of view and make the hydraulic pumping unit an undesired solution especially in sensitive fields that are located near to urban areas or agricultural lands.

The following section discusses the main sources of the problems and suggests some measures to mitigate them.

8.3.1 Noise Protection

It is widely accepted by many designers that noise is inherent to hydraulic systems; therefore, it is important to note that all proposed measures tend to reduce and minimize the noise to an acceptable level rather than drastically cancel it.

The main source of noise in hydraulic systems is the power unit including the electric motor, the pump and the valves. Other components such as the hydraulic cylinder and fluid conductors (e.g. tubing, hose, and fittings) might contribute to the noise generation.

In the electric motor, noise is generated from bearings, rotor/stator assembly and the fan. In the pump, noise does not come only from the bearings of the pumping elements but also due to the pressure fluctuations resulting from the cyclic pumping process. Another source of noise is the coupling between the pump and the motor. For the case of valves, when fluid passes at high velocities through the valve, it results in a severe pressure drop causing dissolved air to form bubbles. Noise occurs when those bubbles collapse. [24]

In general, noise sources can be classified into three main categories: 1) Structure-borne noise, 2) Fluid-borne noise and 3) Air-borne noise. Measures to mitigate each of the list noise categories are listed below:

1) Structure-borne noise

Such noise results from the vibration of the mass of the power unit (electric motor and pump). It can be reduced by using larger motors and pumps running at lower speed. In addition, the power unit should be installed on vibration-damping mounts in order to reduce the vibration and noise generation.

Since the coupling between motor and pump is regarded as a source of noise, one of the solutions is to combine these two components into one single block.

2) Fluid-borne noise

Fluid borne-noise comes from pressure pulsation inside the hydraulic components such as pumps or valves. One of the effective solutions is to install a reflective silencer. The silencer

generates secondary sound waves that are exactly opposite to the original waves in amplitude and frequency.

Another solution is to replace the metal connections of the pump by flexible connections such as rubbers or hoses.

In the case of long tubing or pipes, fluid-borne noise can be reduced by inserting sections of hose at the terminations of these metal tubing in order to isolate the noise.

3) Air-borne noise

Air-borne noise can be minimized by preventing the propagation of the sound waves generated by the pump and motor into the air. This is achieved by submerging the power unit inside the reservoir. Using the technique the surrounding liquid will dampen the generated sound waves and acts as noise isolator between the power unit and the outside atmosphere.

It is important as well to prevent air from being dissolved in the hydraulic fluid in order to avoid cavitation. Therefore, air must be properly separated from the hydraulic fluid by allowing for maximum settling time at the reservoir.[24]

8.3.2 Leaks Mitigation

Similarly to noise, leakages are also considered inherent to hydraulic systems especially when operating under high pressures, which is the case for the hydraulic cylinder. Typical solutions tend to reduce leakage associated to long stroke hydraulic units by maximizing the surface stroke length of the polished rod and reducing the pumping speed. This results in fewer pumping cycles and postponement in the leakage occurrence.

Since the leakage occurrence is inevitable, newer approaches tend to eliminate the environmental hazards of leaks by containing the hydraulic cylinder entirely inside the production tubing. This will ensure the elimination of any external leak points and prevent the propagation of the leaked fluid externally. On the meanwhile, leak detection systems must be implemented in order to warn the operator before the complete failure of the system.

References

1. Lake, L. and Arnold, K. (2007). Petroleum engineering handbook. Richardson, TX: Society of Petroleum Engineers.
2. Herbert Hofstätter. 2016. Artificial Lift Systems. General Introduction lecture notes. Leoben, Austria.
3. Clemens Langbauer. 2017. Artificial Lift Systems Practical. Pump Comparison lecture notes. Leoben, Austria.
4. Sucker rod pumping short course. (2017).
http://docs.wixstatic.com/ugd/f8ee70_d4ba77a8b77e40d898037b28bebad23e.pdf
[Accessed 22 Aug. 2017]
5. Takacs, G. (2015). Sucker-Rod Pumping Handbook.
6. Anon, (2017). Sucker-rod_lift. [online] Available at: http://petrowiki.org/Sucker-rod_lift
[Accessed 22 Aug. 2017].
7. www.slb.com. (2017). Rod pump systems.
8. Petrowiki.org. (2017). Sucker-rod pumping units -. [online] Available at: http://petrowiki.org/index.php?title=Sucker-rod_pumping_units&printable=yes
[Accessed 22 Aug. 2017].
9. www.hdc.ca. (2008). Describe and operate beam pump.
10. Jcpump.net. (2017). JCPump, LLC. - American Made Pump Jack, Pumping Unit.<http://jcpump.net/> [Accessed 22 Aug. 2017].
11. Beck, T. and Peterson, R. (2009). A comparison of the performance of linear actuator versus walking beam pumping systems.
12. Khadav, S., Kumar, R., Kumar, P., Kumar, V., Deo, A., Kumar, P., & Kumar, S. (2016, November 30). New Solutions for Installation of Sucker Rod Pumps in Marginal Field. Society of Petroleum Engineers. doi:10.2118/184202-MS
13. Air balance control for a pumping unit. (1993). Patent No° 5180289.
14. Lufkin conventional & reverse mark pumping units.
<https://www.scribd.com/doc/191418451/Lufkin-Conventional-Installation-Manual>
[Accessed 22 Aug. 2017].
15. Lufkin Mark II Pumping Units.
<https://www.scribd.com/document/30248238/Manual-de-Instalacion-Mark-II>
[Accessed 22 Aug. 2017].
16. Choose the Best Long-Stroke Sucker Rod Pumping System for Your Application.2015.
<http://www.upstreampumping.com/article/production/2015/choose-best-long-stroke-sucker-rod-pumping-system-your-application>.
17. Chang, L., Lin, S. and Zheng, h. (2013). Hydraulic system research of the pumping unit based on electro-hydraulic proportional control technology.
18. Li, Z. and Song, J. (2017). Design and analysis for a new energy-saving hydraulic pumping unit.
19. Hans-Petter.H. (2016). Introduction to Simulink.
20. Fatemeh Fazeli.2016. Analysis and Simulation of a High Performance Wire and Fiber Rope as Continuous Sucker Rod String. Master Thesis, Montanuniversitaat.
21. W. Phillips. Improving the Reliability and Maintenance Costs of Hydraulically Actuated Sucker Rod Pumping Systems. SPE Artificial Lift Conference Colombia, 21-22 May 2013.
22. Beam Lift Tool Box. (2018). Retrieved from
<https://cee.utexas.edu/ce/petex//aids/pubs/beam-lift/toolbox/#torquefactors>

23. Collins, D. (2018). How to Calculate Velocity from Triangular and Trapezoidal Move Profiles. Retrieved from www.linearmotiontips.com/how-to-calculate-velocity/. [accessed 12 May. 2018]
24. Noise control in hydraulic systems. (2018). Retrieved from <http://www.hydraulicspneumatics.com/200/FPE/SystemDesign/Article/False/6461/FP E-SystemDesign>. [Accessed 13 May.2018]
25. Clemens Langbauer.2015. Sucker Rod Anti-Buckling system Analysis. PhD
26. Hydraulic Cylinder with Two-Chamber Snubbers- MATLAB & Simulink- MathWorks Australia. (2018). Retrieved from <https://au.mathworks.com/help/phymod/hydro/examples/hydraulic-cylinder-with-two-chamber-snubbers.html>
27. Kamble. (2018). Actuators in hydraulic system. Retrieved from <https://www.slideshare.net/Ash008/actuators-in-hydraulic-system>. [Accessed on 24 May 2018]
28. Shock Loading Of Hydraulic Cylinders. (2018). Retrieved from <https://www.cylinder.co.uk/glossary/shock-loading-of-hydraulic-cylinders.html> [Accessed on 29 May 2018]

List of Tables

| | |
|---|----|
| Table 1: A Comparison between different Artificial Lift Systems [2] | 3 |
| Table 2: Advantages and Limitations of Sucker Rod Pumping System [1] | 7 |
| Table 3: Technical Data of Available DynaPump Models [16]..... | 16 |
| Table 4: Wellbore Specifications | 30 |
| Table 5: Pump jack Specifications | 30 |
| Table 6: Design Specifications of CSR string and Wire Rope | 32 |
| Table 7: Configuration of main Unit Components – Case Study 3 | 38 |
| Table 8: Configuration of main Unit Components – Case 4 | 41 |
| Table 9: Summary of Results of the Four Case Studies | 51 |
| Table 10: Excel Model for kinematics Calculation of The Conventional Pumping Unit | 66 |
| Table 11: Summary of the Hydraulic System Components | 68 |
| Table 12: Parameter Configuration of Hydraulic Components | 69 |

List of Figures

| | |
|--|----|
| Figure 1. Usage of Artificial Lift Systems Worldwide [3] | 3 |
| Figure 2. Schematic of Conventional Sucker Rod Pumping System [5] | 4 |
| Figure 3: Failure Distribution by Location | 5 |
| Figure 4. Full Pumping Cycle of a Downhole Rod Pump [3] | 6 |
| Figure 5. Pump Card Shapes Analysis [4] | 7 |
| Figure 6. Main Components of Conventional Pumping Unit [14] | 10 |
| Figure 7. Example of Beam-balanced Pumping Unit [10] | 11 |
| Figure 8. Schematic of Air-Balanced Beam Pumping Unit [13] | 11 |
| Figure 9. Main Components of Mark II Pumping Unit [15] | 12 |
| Figure 10. Structure of the DynaPump Unit [5] | 14 |
| Figure 11. 3-Chamber Hydraulic Cylinder [5] | 15 |
| Figure 12. Velocity Profile during a Complete Pumping Cycle [5] | 17 |
| Figure 13. Hydraulic System of Hydraulic Pumping Unit | 18 |
| Figure 14. Hydraulic Control System of the Hydraulic Pumping Unit [17] | 19 |
| Figure 15. Speed Curve of the Pump [17] | 20 |
| Figure 16. Working Principle of the Energy-Saving HPU [18] | 21 |
| Figure 17. Energy-Saving HPU Speed Curve Design [18] | 22 |
| Figure 18: Comparison between Sinusoidal and Trapezoidal Velocity Curves | 23 |
| Figure 19: Double Acting Hydraulic Cylinder with Piston Rod [27] | 24 |
| Figure 20: SRABS Pump Mechanism with a Weight | 28 |
| Figure 21: Polished Rod Motion - Conventional Unit / CSR | 31 |
| Figure 22: Dynamometer Card – Conventional Unit / CSR | 32 |
| Figure 23: Polished Rod Motion - Conventional Unit / Wire Rope | 33 |
| Figure 24: Dynamometer Card - Conventional Unit / WR | 33 |
| Figure 25: String Stretch of continuous ropes [20] | 34 |
| Figure 26: Simulink Blocks Library | 35 |
| Figure 27: Schematic of the Cushioning Device [26] | 36 |
| Figure 28: Schematic of the Hydraulic Pumping Unit Model | 37 |
| Figure 29: Valve Control Signal - Case Study 3 | 39 |
| Figure 30: Block Diagram for Polished Rod Load Simulation | 40 |

| | |
|---|----|
| Figure 31: Polished Rod Load Curve – Hydraulic Unit with CSR String | 40 |
| Figure 32: Valve Control Signal - Case Study 4..... | 41 |
| Figure 33: Polished Rod Load Curve - HPU with Wire Rope | 42 |
| Figure 34: Polished Rod Load Displacement (Left: Case 3 – Right: Case 4) | 43 |
| Figure 35: Velocity Profile (Left: Case 3 – Right: Case 4)..... | 44 |
| Figure 36: Hydraulic Pump Flow Rate - Case Studies 3 & 4 | 46 |
| Figure 37: Hydraulic Pump Pressure – Case Studies 3 & 4 | 46 |
| Figure 38: Power Consumption of the Hydraulic Unit (Left: CSR string /Right: Wire Rope) .. | 47 |
| Figure 39: Polished Rod Displacement of Case Study 1 & 3 | 48 |
| Figure 40: Polished Rod Displacement of Case Study 2 & 4 | 49 |
| Figure 41: Polished Rod Velocity - Case Study 1 & 3 | 50 |
| Figure 42: Polished Rod Velocity - Case Study 2 & 4 | 50 |
| Figure 43: Power Consumption of the Modeled Pumping Unit..... | 51 |
| Figure 44: S-curve Velocity Profile [23]..... | 54 |
| Figure 45: Force Calculation Process under Double and Single well Conditions | 64 |
| Figure 46: Calculation Process of Hydraulic Parameters | 65 |
| Figure 47: Polished Rod Data Conversion & Implementation into the Excel Calculation Model | 67 |

Abbreviations

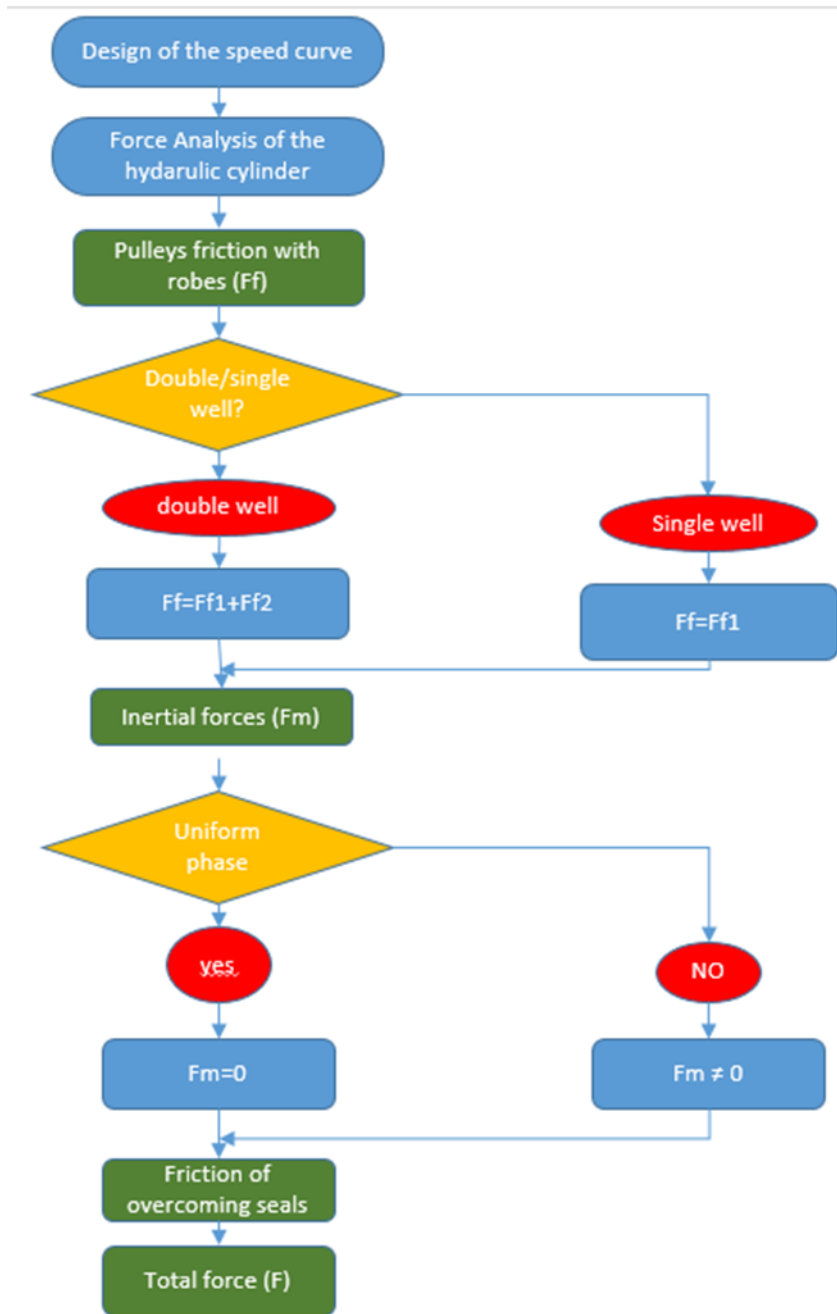
| | |
|-------|---------------------------------|
| API | American Petroleum Institute |
| BPD | Barrel per Day |
| C | Degrees Centigrade |
| cp. | Centi-Poise |
| CSR | Conventional Sucker Rod |
| ESP | Electric Submersible Pumps |
| F | Force |
| ft. | Foot |
| HPU | Hydraulic Pumping Unit |
| in. | Inch |
| kPa | Kilo-Pascal |
| ksi | Kilo Pounds per Square Inch |
| lb | Pound |
| m. | Meter |
| MD | Measured Depth |
| MPa | Mega-Pascal |
| MTBF | Mean Time between Failure |
| OPEX | Operating Expense |
| PCP | Progressive Cavity Pump |
| psi | Pounds per Square Inch |
| SF | Safety Factor |
| SPM | Strokes per Minute |
| SR | Sucker Rod |
| SRABS | Sucker Rod Anti-Buckling System |

SRP Sucker Rod Pump

TVD True Vertical Depth

Appendices

Appendix A



1

Figure 45: Force Calculation Process under Double and Single well Conditions

F_{f1} , F_{f2} , F_f : Friction forces between wire ropes and pulleys.

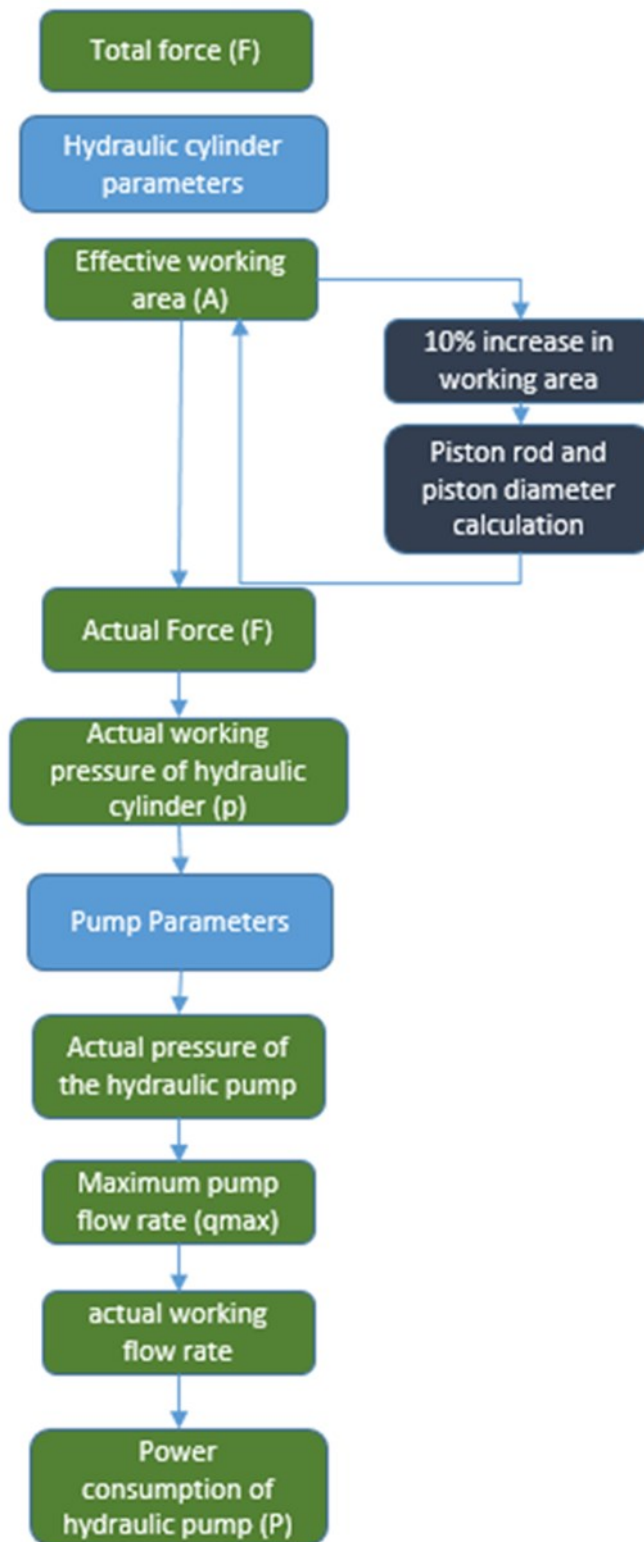


Figure 46: Calculation Process of Hydraulic Parameters

Appendix B

Table 10: Excel Model for kinematics Calculation of The Conventional Pumping Unit

| Torque Factors & Kinematics | | Enter Data in Yellow Fields | | | | | | | | | | | | | | | |
|-----------------------------|-----------|--|---|--------|--------|------|-------|--|-----------------|-------------------|-------------------------------------|------------|------------|---------------------------|---------------------|--------------------------|---------------|
| Data | | Unit | C320D-256-144 | | | | | | | | | | | | | | |
| A | 185.2 | Inches | Gear Box | 320000 | In-lbf | | | | | | | | | | | | |
| P | 133.9 | Inches | Beam | 25600 | lbf | | | | | | | | | | | | |
| C | 111.2 | Inches | | | | | | | | | | | | | | | |
| I | 111 | Inches | Zero crank angle is during the up stroke. | | | | | | | | | | | | | | |
| K | 160 | Inches | | | | | | | | | | | | | | | |
| R | 41.9 | Inches | | | | | | | | | | | | | | | |
| crank rotation | 1 | positive 1 is CW, negative 1 is CCW with horse head on the right | | | | | | | | | | | | | | | |
| Phi | 0.77 | | | | | | | | | | | | | | | | |
| Cb | 1.37 | Speed | 5 | spm | | | | | | | | | | | | | |
| Cf | 0.59 | | | | | | | | | | | | | | | | |
| Crank | | Polished Rod Torque | | | | | | | | | | | | | | | |
| Angle-deg | Angle-rad | Position | Factor (in) | beta | h | c | alpha | | Position (inch) | Velocity (ft/sec) | Acceleration (ft/sec ²) | Time (sec) | Load (lbs) | Well Load Torque (in-lbs) | CBE Torque (in-lbs) | Gear Box Torque (in-lbs) | Work (ft-lbf) |
| 0.00 | 0.00 | 0.00 | -9.80 | 1.13 | 133.04 | 1.37 | 3.27 | | 0.48 | 0.00 | 0.00 | 0.00 | 8777.91 | -80550.88 | 0.00 | -80550.88 | |
| 5.00 | 0.09 | 0.00 | -1.10 | 1.11 | 130.10 | 1.37 | 3.16 | | 0.01 | -0.24 | -1.44 | 0.00 | 8777.91 | -9025.45 | 72957.51 | -81992.96 | -347.87 |
| 10.00 | 0.17 | 0.00 | 7.99 | 1.08 | 127.40 | 1.37 | 3.04 | | 0.30 | 0.15 | 2.33 | 0.00 | 8992.74 | 65659.36 | 145359.78 | -79700.42 | 220.18 |
| 15.00 | 0.26 | 0.01 | 17.32 | 1.06 | 124.98 | 1.36 | 2.92 | | 1.41 | 0.55 | 2.41 | 0.00 | 9557.91 | 147102.72 | 216655.76 | -69553.05 | 852.73 |
| 20.00 | 0.35 | 0.02 | 26.72 | 1.04 | 122.88 | 1.35 | 2.81 | | 3.33 | 0.96 | 2.46 | 0.01 | 11419.88 | 242015.35 | 286302.87 | -44287.52 | 1679.82 |
| 25.00 | 0.44 | 0.04 | 35.97 | 1.02 | 121.13 | 1.34 | 2.69 | | 6.07 | 1.37 | 2.45 | 0.02 | 12366.44 | 392842.04 | 353771.04 | 39071.00 | 2713.00 |
| 30.00 | 0.52 | 0.07 | 44.86 | 1.01 | 119.76 | 1.32 | 2.57 | | 9.60 | 1.77 | 2.38 | 0.04 | 14765.52 | 532328.59 | 418546.79 | 113781.80 | 3995.81 |
| 35.00 | 0.61 | 0.10 | 53.14 | 1.00 | 118.79 | 1.30 | 2.45 | | 13.88 | 2.14 | 2.25 | 0.07 | 14312.40 | 759610.77 | 480137.16 | 279473.62 | 5192.34 |
| 40.00 | 0.70 | 0.13 | 60.58 | 0.99 | 118.23 | 1.27 | 2.33 | | 18.85 | 2.48 | 2.06 | 0.10 | 16329.14 | 836712.12 | 538073.39 | 296638.73 | 6343.46 |
| 45.00 | 0.79 | 0.17 | 66.99 | 0.99 | 118.11 | 1.24 | 2.21 | | 24.42 | 2.79 | 1.82 | 0.13 | 16780.88 | 1060315.47 | 591914.55 | 468400.92 | 7689.89 |
| 50.00 | 0.87 | 0.21 | 72.21 | 0.99 | 118.42 | 1.21 | 2.09 | | 30.50 | 3.04 | 1.53 | 0.17 | 16239.53 | 1175677.53 | 641250.89 | 534426.64 | 8368.78 |
| 55.00 | 0.96 | 0.26 | 76.17 | 1.00 | 119.15 | 1.17 | 1.98 | | 36.99 | 3.24 | 1.20 | 0.21 | 15992.46 | 1198882.10 | 685706.92 | 513175.18 | 8891.53 |
| 60.00 | 1.05 | 0.30 | 78.84 | 1.01 | 120.30 | 1.13 | 1.86 | | 43.76 | 3.39 | 0.87 | 0.26 | 16733.56 | 1216641.62 | 724944.31 | 491697.31 | 9218.30 |
| 65.00 | 1.13 | 0.35 | 80.25 | 1.03 | 121.84 | 1.10 | 1.75 | | 50.71 | 3.48 | 0.53 | 0.30 | 18397.70 | 1302766.94 | 758664.44 | 544102.50 | 10173.94 |
| 70.00 | 1.22 | 0.40 | 80.51 | 1.04 | 123.74 | 1.06 | 1.65 | | 57.73 | 3.51 | 0.22 | 0.35 | 16759.12 | 1440900.04 | 786510.67 | 654299.37 | 10286.93 |
| 75.00 | 1.31 | 0.45 | 79.74 | 1.07 | 125.98 | 1.02 | 1.54 | | 64.73 | 3.50 | -0.07 | 0.40 | 14680.09 | 1296422.84 | 808870.32 | 487882.52 | 9171.18 |
| 80.00 | 1.40 | 0.50 | 78.09 | 1.09 | 128.52 | 0.98 | 1.44 | | 71.62 | 3.45 | -0.32 | 0.45 | 13671.10 | 1108053.35 | 824376.26 | 283677.10 | 8144.46 |
| 85.00 | 1.48 | 0.54 | 75.72 | 1.12 | 131.33 | 0.95 | 1.35 | | 78.34 | 3.36 | -0.53 | 0.50 | 12666.42 | 997321.19 | 833908.20 | 163412.99 | 7375.42 |
| 90.00 | 1.57 | 0.59 | 72.79 | 1.15 | 134.36 | 0.91 | 1.26 | | 84.82 | 3.24 | -0.70 | 0.54 | 11890.69 | 887058.84 | 837993.59 | 49955.25 | 6639.50 |

Appendix C

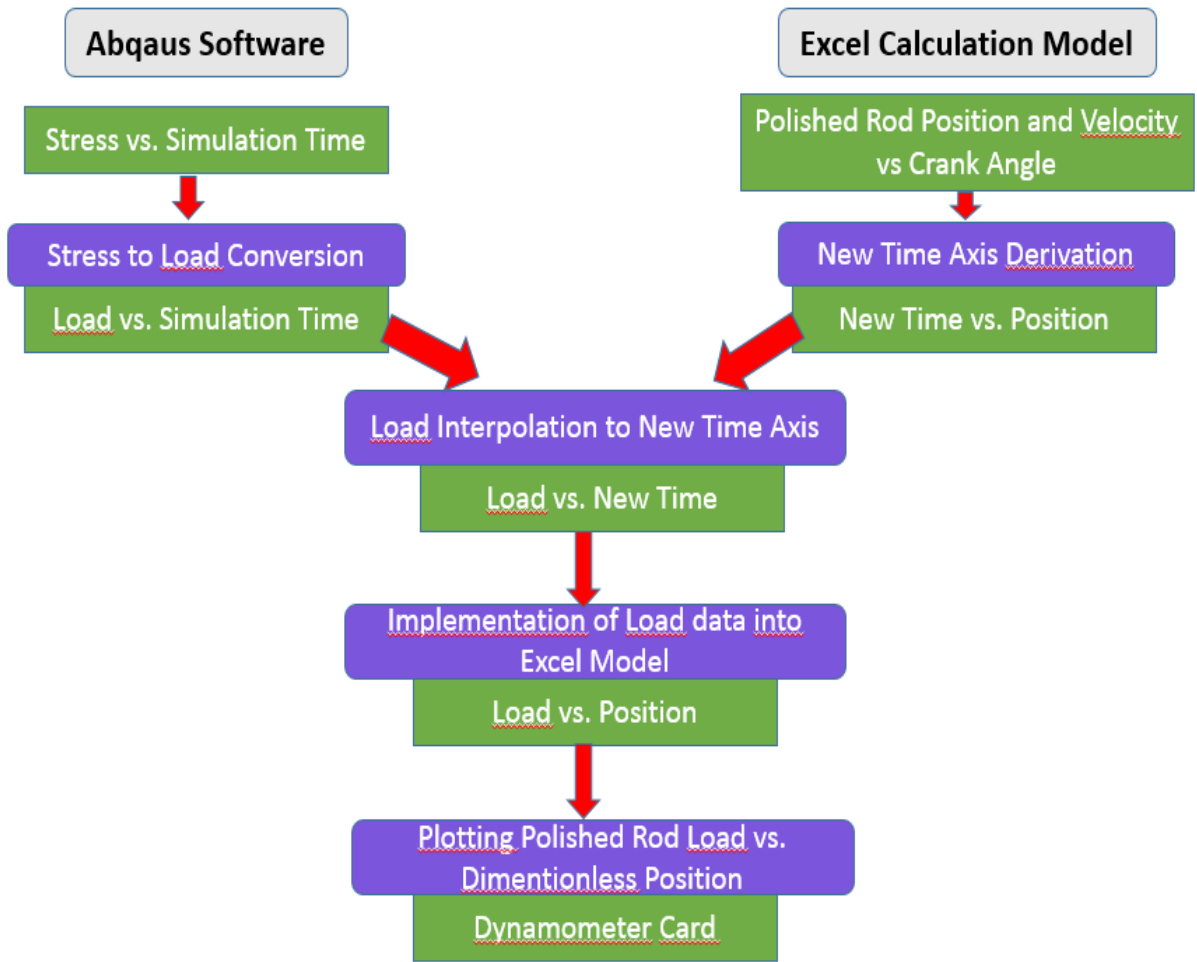



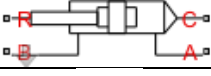














Figure 47: Polished Rod Data Conversion & Implementation into the Excel Calculation Model

Appendix D

Table 11: Summary of the Hydraulic System Components

| Component | Symbol | Function |
|---|---|---|
| Angular velocity Source |  | Supplies the system with the primary energy in form of rotational velocity |
| Variable displacement pump |  | Converts mechanical rotational energy into hydraulic energy in form of rate and pressure |
| 4-way directional valve |  | Directs the pumped fluid to different sides of the hydraulic cylinder |
| Double-Acting Hydraulic Cylinder |  | Converts hydraulic energy into mechanical translational motion |
| Mass |  | Represents the weights of auxiliary components |
| Translational Damper |  | Indicates an error message when unrealistic acceleration magnitudes occurs |
| Translational Spring |  | Provides damping force to prevent velocity fluctuations within the system |
| Force Source |  | Generates a force that is proportional to its input signal |
| Signal builder |  | Creates and defines input signals (waveforms) to control operations of some components |
| Mechanical translational reference |  | Represents a reference point or a frame to translational components |
| Mechanical rotational reference |  | Represents a reference point or a frame to rotational components |
| Fixed Orifice |  | Constant area orifice through which the flow rate is controlled by the fluid pressure across it |
| Check Valve |  | Allow fluids to flow in only one direction |
| PS Constant |  | Generates a physical signal having a constant value |
| Hydraulic fluid |  | Provides fluid properties: kinematic viscosity, density, bulk modulus... |
| Simulink-PS converter |  | Converts input Simulink signal into physical signal |

Appendix E

Table 12: Parameter Configuration of Hydraulic Components

| Component | Parameter | Unit | Value | |
|-------------------------|-----------------------|----------------------|--------------|--------------|
| | | | Case Study 3 | Case Study 4 |
| Hydraulic Pump | Max displacement | [(l/rev)] | 2 | 2 |
| | Rotation per minute | [RPM] | 1200 | 1200 |
| | Nominal pressure | [MPa] | 7.2 | 7.2 |
| 4-way Directional Valve | Maximum orifice area | [cm ²] | 10 | 10 |
| | Discharge coefficient | [-] | 0.7 | 0.7 |
| Hydraulic Cylinder | Piston stroke | [m] | 8 | 8 |
| | Piston area A | [cm ²] | 24 | 24 |
| | Piston area B | [cm ²] | 19 | 19 |
| Translational Damper | Damping Coefficient 1 | [N/(m/s)] | 20 | 10 |
| | Damping Coefficient 2 | [N/(m/s)] | 2 | 2 |
| Translational Spring | Spring Rate | [N/m] | 0.1 | 0.1 |
| Fixed Orifice | Orifice Area | [cm ²] | 0.43 | 1 |
| Check Valve | Cracking pressure | [KPa] | 30 | 30 |
| PS Constant | Constant 1 | [-] | 1 | 1 |
| | Constant 2 | [-] | 10 | 12 |
| Hydraulic fluid | Density | [Kg/m ³] | 866.8 | 866.8 |
| | Viscosity | [cSt] | 38.7 | 38.7 |